

# Did the Black-Mat Impact/Airburst Reach the Antarctic? Evidence from New Mountain Near the Taylor Glacier in the Dry Valley Mountains

W. C. Mahaney,<sup>1,\*</sup> David H. Krinsley,<sup>2,†</sup> Michael W. Milner,<sup>3</sup>  
Robert Fischer,<sup>2</sup> and Kurt Langworthy<sup>2</sup>

1. Quaternary Surveys, 26 Thornhill Avenue, Thornhill, Ontario L4J 1J4, Canada; and Department of Geography, York University, 4700 Keele Street, Toronto, Ontario M3J 1P3, Canada; 2. Department of Geological Sciences, University of Oregon, Eugene, Oregon 97403, USA; and Center for Advanced Materials Characterization in Oregon (CAMCOR), University of Oregon, Eugene, Oregon, 97403, USA; 3. MWM Consulting, 182 Gough Avenue, Toronto, Ontario M4K 3P1, Canada

## ABSTRACT

Detailed microscopic investigations of horizons in a surface paleosol, part of a pedostratigraphic stack of tills at New Mountain, Antarctica, dated to the middle Miocene climatic optimum event (ca. 15 Ma), suggest not only that the paleoclimate history of the continent can be read from stratigraphic layers within paleosols but also that records of cosmic events may lie embedded in coatings on sand clasts resident in paleosols. Recent microscopic and chemical data from sands in the upper horizons of a surface paleosol (Ant-828), adjacent to the Taylor Glacier, contain Fe and Na coatings surfaced with cosmic signatures including welded and shock-melted grains, opaque carbon coatings, microfeature stack of cards, Fe spherules, solubilized grain surfaces with streams of melted skin, a grain carrying an Ir signature, rare earth elements elevated above crustal averages, and slightly elevated Pt/Pd ratios. The projected link to the probable black-mat event of 12.8 ka is reinforced by the presence of fresh opaque carbon and other cosmic signatures on grain surfaces that overlie well-weathered grain features, presumably weathering from middle Miocene time near today. Evidence of CO<sub>2</sub> and NO<sub>x</sub> accumulations dated to 12.9 ka in the Taylor Ice Dome suggest that the black-mat impact/airburst of the same time line as the Younger Dryas boundary may have reached across South America and the Pacific Ocean to the Dry Valley Mountains of Antarctica.

## Introduction

Black-mat sediments have been discovered on every continent except Australia, New Zealand, and Africa, with the main body of evidence for a cosmic impact/airburst so far limited to North, Central, and South America, Greenland, western and central Asia, and Europe. The principle line of evidence of a cosmic collision comes from thin (2–3 cm thick) black beds comprising variable amounts of carbon; charcoal; welded/contorted, shock-melted grains of nearly every lithology, often accompanied by Pt within meteoric impact limits (Petaev et al. 2013); and Co/Fe, Cu/Fe, and rare earth element (REE) concentrations above crustal averages (table 1). Impact/airburst evidence is

not limited to black-mat beds in lacustrine and alluvial sediment and in ice cores where significant finds have been made but is also found in paleosols and in weathering rinds recovered from paleosol surfaces (Mahaney and Keiser 2013; Mahaney et al. 2013*b*, 2016*a*, 2016*b*, 2017). Many sites have been dated by accelerator mass spectrometry radiocarbon to within ± 150 y of a mean date of 12.8 ky BP (Kennett et al. 2015; Wolbach et al. 2018*a*, 2018*b*). Because no impact crater has been identified, and since all black-mat evidence lies well beyond the reported collision of Earth with the comet Encke (Napier 2010; southern Manitoba), most workers refer to an airburst rather than impact of cometary material.

Opposition to a cosmic origin for the Younger Dryas (YD) resurgence of ice following the Bølling-Allerød warming after the last ice age has been swift and strong (van der Hammen and van Geel 2008;

Manuscript received January 28, 2018; accepted February 1, 2018; electronically published March 15, 2018.

\* Author for correspondence; email: arkose41@gmail.com.

† Deceased November 5, 2017.

[The Journal of Geology, 2018, volume 126, p. 285–305] © 2018 by The University of Chicago.  
All rights reserved. 0022-1376/2018/12603-0002\$15.00. DOI: 10.1086/697248

Broecker et al. 2010), with a number of climatic, archaeological, and geological authorities arguing that the YD boundary (YDB) does not correlate exactly with the demise of megafauna, the disappearance of the Clovis people in North America, and/or the release of meltwater from the Laurentian Ice Sheet, the latter event possibly connected with a disturbance of the thermohaline circulation of the West Wind Drift in the Atlantic Ocean. Some workers have argued that  $^{14}\text{C}$  dating of the black mat is diachronous across the sites investigated (Meltzer et al. 2014), an assertion refuted by Kennett et al. (2015), who showed that the dates were in fact isochronous across the 12.8-datum plane with narrow standard deviations.

Evidence that the cosmic airburst reached deep into the Southern Hemisphere is complicated by the fact that land surfaces, relative to the Northern Hemisphere, are restricted, and fewer workers are resident in the Southern Hemisphere to search for likely sites that may contain the relevant affected sediments. In South America, strong, irrefutable evidence of the black mat comes from the Mérida Andes in northwestern Venezuela (Mahaney et al. 2013a) and from central Peru; another likely site is at Lake Potrok in Argentina, within ~1500 km of Antarctica (Kyeong Kim, Korea Institute of Geoscience and Mineral Resources, personal communication to W. C. Mahaney, 2015, 2016). While Antarctica is not a likely locality for resident black-mat sediment to be found, recent recovery of burn proxies, especially C-CO<sub>2</sub>-NO<sub>x</sub>, in a core retrieved from the Taylor Ice Dome (Brook et al. 2015) suggests that other evidence may lie in nearby resident paleosols that date to the time of the middle Miocene climatic optimum (MMCO), dated with  $^{10}\text{Be}$  to ~15 Ma for the upper paleosol at New Mountain and 17 Ma for the middle paleosol. These dates are supported by a nitrate inventory of ~18 Ma (Graham et al. 2002). Previous work in Antarctica has shown that weathering histories can be reconstructed from sediment retrieved not only from ancient soils—paleosols (Mahaney et al. 2001)—but also from even older weathering rinds dating to the time of the alpine glaciation before the buildup of the Inland Ice Sheet (Mahaney and Schwartz 2016). Weathered sediment from the surface of a resident paleosol of post-MMCO age carries sands bearing a cosmic signature that closely resembles black-mat grains studied elsewhere (Mahaney et al. 2013a). Alternative to a projected black-mat correlation, it could be that the present paleosol evidence points to meteor ablation at some time between the MMCO and the present, but the affinity to a dated ice lens in the Taylor Ice Dome (Brook et al. 2015) suggests, but does not prove, a possible coeval event.

## Regional Geology

The Transantarctic Mountains, including the Taylor Glacier–New Mountain area (fig. 1), comprise a complex of sedimentary layers overlying Antarctic basement rock of granites and gneisses. The sedimentary layers include the Beacon Supergroup (Stewart 1934; Shaw 1962), which includes mainly arkosic sandstones locally intruded by doleritic dikes and sills (Ferrar dolerite). Moraines at New Mountain carry this mix of sandstone, dolerite, granite, and gneiss, with granite and gneiss constituting the main lithologies in the field area. The topography alternates from steep slopes and drainage divides to benches, producing a setting similar to the landscape of South Africa, where these surface features originally formed under arid climates (Campbell and Claridge 1987; Mahaney et al. 2001). In the McMurdo area, centers of volcanism dating from 10 to 15 Ma (Armstrong 1978) are only slightly modified by glacial and mass-wasting activity. Even Mount Terror, in the Ross Island area, retains a conical shape indicative of little modification by glacial/mass-wasting processes.

Granitic basement rocks form erosion surfaces over a broad swath of the Transantarctic Mountains overlain by continental sandstone of Devonian to Jurassic age, originally named the Beacon sandstone (Ferrar 1907), from outcrops near the Taylor Glacier. These sandstones were later integrated to include all grades of clastic rocks from conglomerates to siltstone transitioning upward into thick, quartz-rich sandstone of Devonian age, which comprises some of the sediments examined here. As suggested by Campbell and Claridge (1987), Barrett (1981), and Bradshaw (2013), some of these sediments were sourced from basement rocks of East Antarctica.

According to a number of workers, the initiation of glaciation in East Antarctica began during the late Oligocene to early Miocene (Marchant et al. 1993; Lewis et al. 2007; Bo et al. 2009; Denton et al. 2010; Anderson et al. 2011; Passchier 2011; Mahaney et al. 2014; Mahaney 2015) and possibly earlier, in the Eocene (Wilson 1973). Whatever the time of initiation, glaciation began in the mountains, with warm-based ice developing similar to what exists today in middle-latitude areas (Campbell and Claridge 1987) and a slow change over to cold-based ice at some time in the middle Miocene (Warny et al. 2009). During parts of the Quaternary, the climate may have been colder than today's, and the degree to which this affected the mass balances of the continental versus alpine ice is unknown. Moraines at Aztec Mountain and in New Mountain embayments are thought to have been deposited by cold-based ice at some point during the MMCO, as described by Mahaney et al.

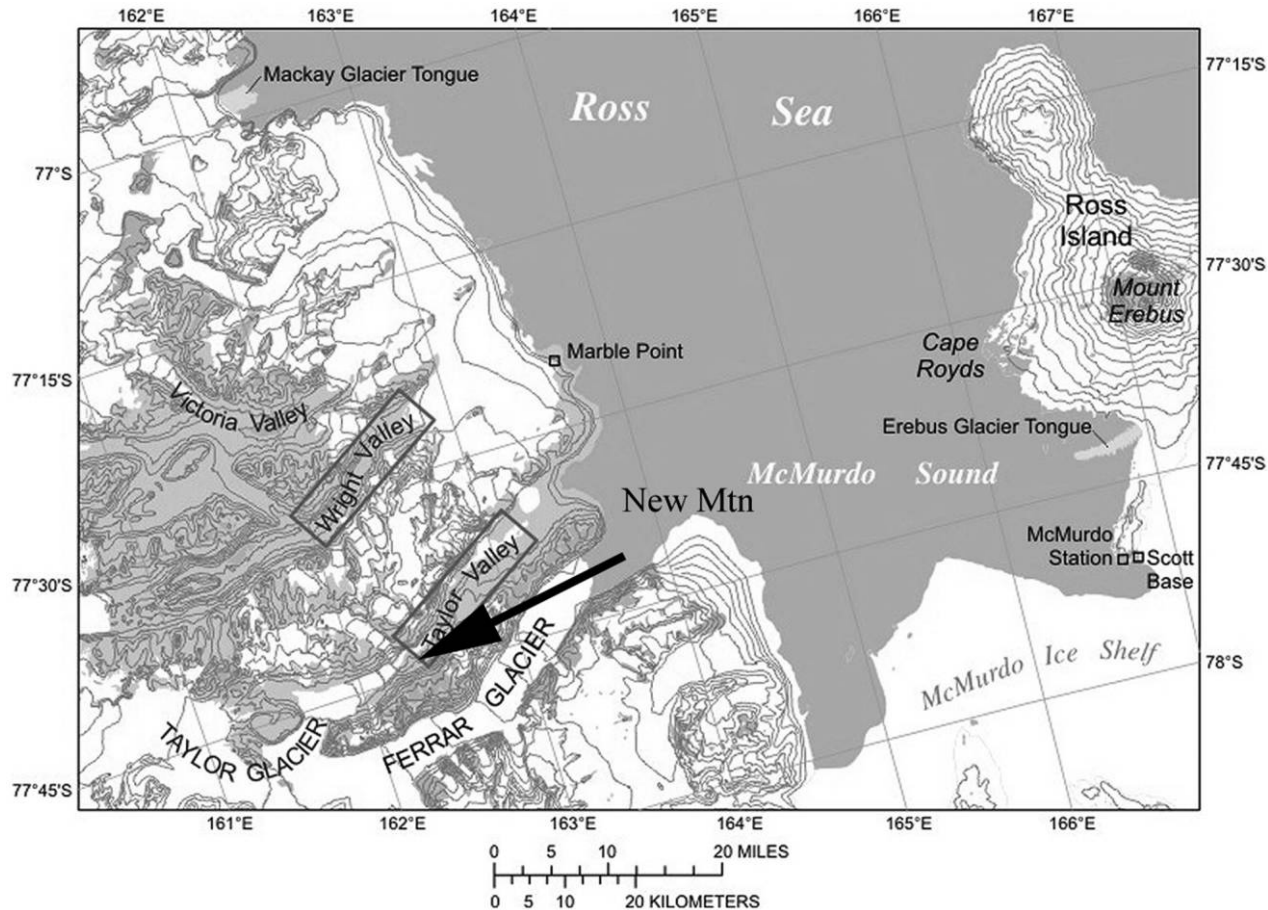


**Figure 1.** Location of Ant-828 in the Dry Valley Mountains, Antarctica. A color version of this figure is available online.

(2001). Incursions of ice from outlet glaciers of the Inland Ice Sheet that invaded elevated benches are thought to have been cold based, their velocities produced by plastic deformation rather than basal sliding, which protected rather than eroded underlying moraine deposits (Owen et al. 2009). Alternatively, the underlying substrate may have been frozen, protecting it from erosion, as attested to by the excellent preservation of buried moraines and paleosols formed within, all of which argues for incursions of cold-based ice, the deposit surface armored against erosion.

Evidence for mass-budget changes of the Taylor Glacier producing periodic incursions of ice overtopping divides and flowing into embayments is evident from areas such as New Mountain and Aztec Mountain, with places like New Mountain showing evidence of multiple events starting sometime in the middle Miocene (Mahaney et al. 2001). Each moraine deposition event at New Mountain was followed by ice withdrawal and then by weathering and soil devel-

opment, with each soil morphogenesis event followed by changes of mass balance and renewed incursion of ice and deposition of moraine, followed again by renewed soil morphogenesis. Each paleosol concentrated salt in lower horizons overlain with higher Fe in upper horizons, judging by field colors taken at the time of collection and by salt and Fe concentrations recovered from profiles after laboratory analysis (Mahaney et al. 2001, 2009). Weathering of pebble pavements lacing the surfaces of these multistory paleosols represents a long middle to late Neogene time span not interrupted by subsequent incursions of ice from the nearby Taylor Glacier (fig. 1). Weathering of pebble clasts presumably progressed along with weathering of associated deposits producing the paleosols, as with the Ant-828 profile discussed here.

The paleosol in the Ant-828 moraine belongs to the cold-desert class of Antarctic soils identified by Campbell and Claridge (1987) here and elsewhere (Bockheim 2007, 2013; Mahaney et al. 2009). Similar

to that of other paleosols at New Mountain and Aztec Mountain, the paleosol moisture regime in Ant-828 is classed as xerous to subxerous, significantly drier than that in pedons of coastal Antarctica, an area with warmer temperatures and higher precipitation (Campbell and Claridge 1987). Infrequent summer snowfall tends to melt and wet pebble pavements and upper horizons of the paleosol bodies, producing high-salinity liquid water that may exist in intergranular films (Ugolini and Anderson 1973; Cuffey et al. 2000; Wynn-Williams and Edwards 2000), thus allowing weathering to continue at temperatures below 0 and provide nutrients for microbe growth. Ugolini and Anderson (1973) showed that during intense freezing episodes, ionic transfer in saline solution may occur through coatings on sand grains of all grades sizes. Lithology within the Ant-828 paleosol is comprised of minor dolerite and sandstone plus significant granite and gneiss.

### Methods

**Field Sedimentary Analysis.** The Ant-828 section is located in an embayment at New Mountain (fig. 1). Excavation of the site revealed a pedostratigraphic succession of tills (fig. 2) deposited at various times during the MMCO, when ice invaded the embayment following expansion of the Taylor Glacier. The samples under analysis here are in the upper horizons of the youngest deposit (see Mahaney et al. 2014 for location of sites) in the succession, the profile shielded somewhat by a ~5-cm-thick pebble pavement, a situation similar to the older Ant-831 section, results of which were discussed by Mahaney and Schwartz (2016).

The site, excavated to just above permafrost, was sectioned to expose in situ sediment. The paleosol horizon descriptions reported here (fig. 2) are genetic, following horizon designations used previously by Mahaney et al. (2009) and adopted from NSSC (1995). As with all paleosol sections analyzed, the usual horizon downward succession follows Fe-rich material underlain with salt-rich sediment, or Cox/Cz horizons, following the US soil classification systems (NSSC 1995; Birkeland 1999; Soil Survey Staff 1999). The Cox designation is used when the sediment color (Oyama and Takehara 1970) is stronger than 10YR 5/4 (Birkeland 1999). The “u” designation in the C horizon nomenclature refers to unweathered sediment (Hodgson 1976).

**Laboratory Analytical Analysis.** Samples were air-dried and sieved to separate pebble-grade material from the <2-mm fraction comprising the bulk sediment sample. The bulk sample was subsampled to

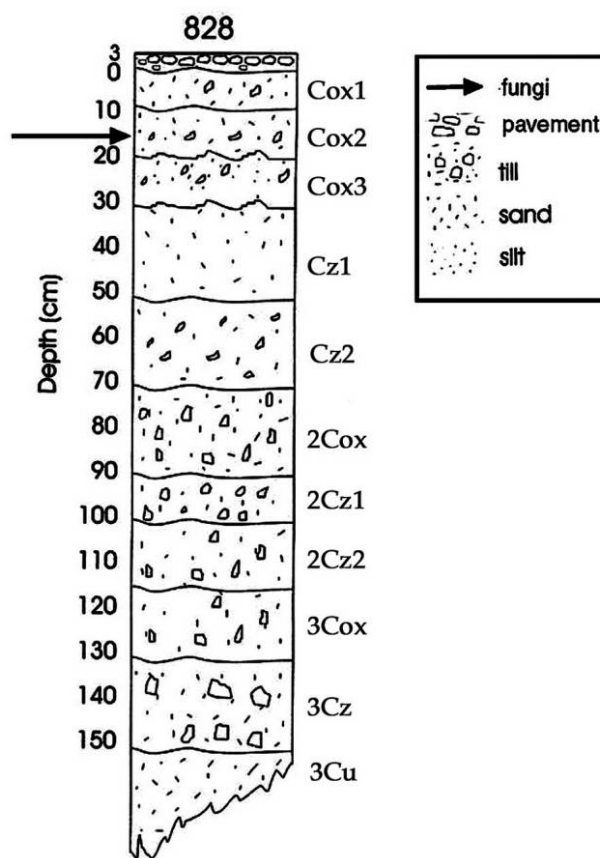


Figure 2. Ant-828 pedostratigraphic paleosol section.

provide 10 g of material to measure the water content, the air-dry weight/oven-dry weight used to determine a moisture factor, which was then used to determine the air-dry equivalent of a 50-g oven-dry sample following ASTM procedures. This air-dry equivalent weight was used to determine the particle size analysis of each sample. Sample preparation involved very light sonication to clean sands, but, given the low or nil organic content, the samples were not subjected to 30% H<sub>2</sub>O<sub>2</sub>, and, given the low clay content, Na-pyrophosphate was not employed for deflocculation. Samples were wet-sieved to separate sand from silt plus clay, and the sands were dried at 110°C and sieved to weigh out the five sand fractions, the coarse (2000–250 μm) and fine (250–63 μm) retained for microscopic analysis. Grains were handpicked with a fine needle from these sand splits, fixed to stubs either with colloidal glue or on sticky tape, and analyzed without coating on a Hitachi scanning electron microscope (SEM), model S-4500. Other grains were analyzed on the same Hitachi SEM and coated with carbon or Au. Still other samples were run on an FEI dual-beam focused ion beam (DB-FIB). Rare earth elements were analyzed on the bulk <2-mm fraction at

the former SLOWPOKE nuclear reactor at the University of Toronto; appropriate standards were used (Hancock 1984; Harrison and Hancock 2005). Platinum determinations were made using fire-assay mass spectrometry on the <177- $\mu\text{m}$  fraction of samples at Activation Laboratories, Ancaster, Ontario, Canada.

## Results

**The Profile.** The Ant-828 profile is one of three sections sampled in the area of New Mountain near the Taylor Glacier. The site is located in an embayment periodically invaded by the Taylor Glacier just before or during the MMCO. The three lithological divisions in the section (fig. 2), designated by Arabic numerals, represent three ice intrusions, each separated by an estimated 1 million years of time; the uppermost profile (unit 1, unmarked by convention) is estimated to have weathered over the past ~15 Ma, but under a dry-cold climate. Each profile within this pedostratigraphic complex contains sets of Cox over Cz horizons, representing oxidized sediment over salt-rich material, as first demonstrated and discussed by Mahaney et al. (2001). Because the time allotted for weathering of each profile was much longer for the surface pedon in the pedostratigraphic section, it is the thickest entity, with greatest subdivision of the Cox group of horizons. In addition to a  $^{10}\text{Be}$  date of ~15 Ma (Graham et al. 2002) for these surface horizons in Ant-828 and a neighboring section in Ant-829, the middle profile (unit 2) in Ant-828 yields a  $^{10}\text{Be}$  age of 17 Ma. In comparison, nitrate ages yield an average age of ca. 18 Ma. In addition, an older alpine moraine (Ant-831) dated with extractable Fe concentrations (Mahaney et al. 2009) suggests that the latter is older, possibly of late Oligocene/early Miocene age (Mahaney and Schwartz 2016).

These profiles do not fit easily into the US soil taxonomy with pavement/Cox/Cz/Cu profiles. Lacking any organic accumulations to build Ah horizons, and because weathering is not advanced enough to produce B horizons, a C complex of weathered sediment plus a buildup of secondary salts, and unweathered C horizons (Cu), these paleosols are essentially weathered mineral bodies. Such paleosols are assigned horizon designations based on degree of chemical alteration and incorporation of secondary salts, the latter mostly accumulated nitrates from marine sources (Claridge and Campbell 1968; Claridge 1977; Campbell and Claridge 1987).

**SEM Analysis and Energy-Dispersive Spectrometry (EDS) Chemistry.** Sand- and silt-size particles are found randomly scattered, some welded to very coarse, small pebble-size granite and felsic gneiss

and others mixed with glass-like carbon and spheroids, dominantly composed of Fe, Si, and Al, as shown with the light microscope photomicrograph in figure 3. The image in figure 3 also shows variable thicknesses of C-rich and Fe-Si-rich coatings (arrows) fused to coarse sand grains surrounded by a grape-like string of spherules that are slightly out of focus, the sands of felsic gneiss and granite typical of grains imported from the Inland Ice Sheet during the MMCO or earlier. This arrangement of opaque and glassy carbon forms a "thread" or grapevine of nodules in which "rod-like forms" lie welded together with adjacent spheroids (arrows), as is common in the black-mat encrusted material comprising stack-of-cards microfeatures (see Mahaney et al. 2014).

Representative grains with variable coatings, as shown in figure 4 and some of the later figures, show shrinkage cracks in coatings, somewhat akin to a stack of cards but most likely the result of cooling after transport. The one microfeature similar to opaque carbon coatings resulting from the black-mat airburst is variable tones in the coatings, the result of Fe-Si distributions, as confirmed by EDS. Figure 4 highlights representative grains recovered from the Cox1' horizon in the Ant-828 paleosol, all coated with variable thicknesses of Ca, Mg, P, Fe, Ti, Cl, and Ir, some no doubt mixed with either glass-like material and/or melted Si and Al. An SEM image of a clast (fig. 5A) reveals a highly melted and molded fresh surface, the grain emitting an albite signature with a smooth, relatively fresh surface. The EDS analysis of the sample reveals only trace concentrations of Fe, P, and Mg, with very minor oxygen (fig. 5B). Approximately 50% of crystals in the one horizon are consistent with melting and mixing of heterogeneous material, followed by cooling too rapid to allow crystallization of Fe, for example, which is immiscible in Si.

The rough texture of the spheroids in figure 3 may have resulted from temperature variability of incoming ejecta from a local airburst and/or from wildfires in a distant locale far north of Antarctica, the latter hypothesis discussed by Wolbach et al. (2018a). The arrow in figure 5A shows an oriented, quench-textured crystal that possibly formed parallel to the direction of travel, which is typical for other YDB sites and similar to five sites in the United States (Arizona, California, Missouri, Ohio, and South Carolina), one in Alberta, Canada, and three in Europe (Germany, Belgium, and the Netherlands; Firestone et al. 2007a, 2007b; Wittke et al. 2013).

Shock melting dominates in figures 6A and 7A, with variable degrees of grain destruction from extreme to slight. Figure 6A carries an example of extreme melting that resembles shock-melted quartz

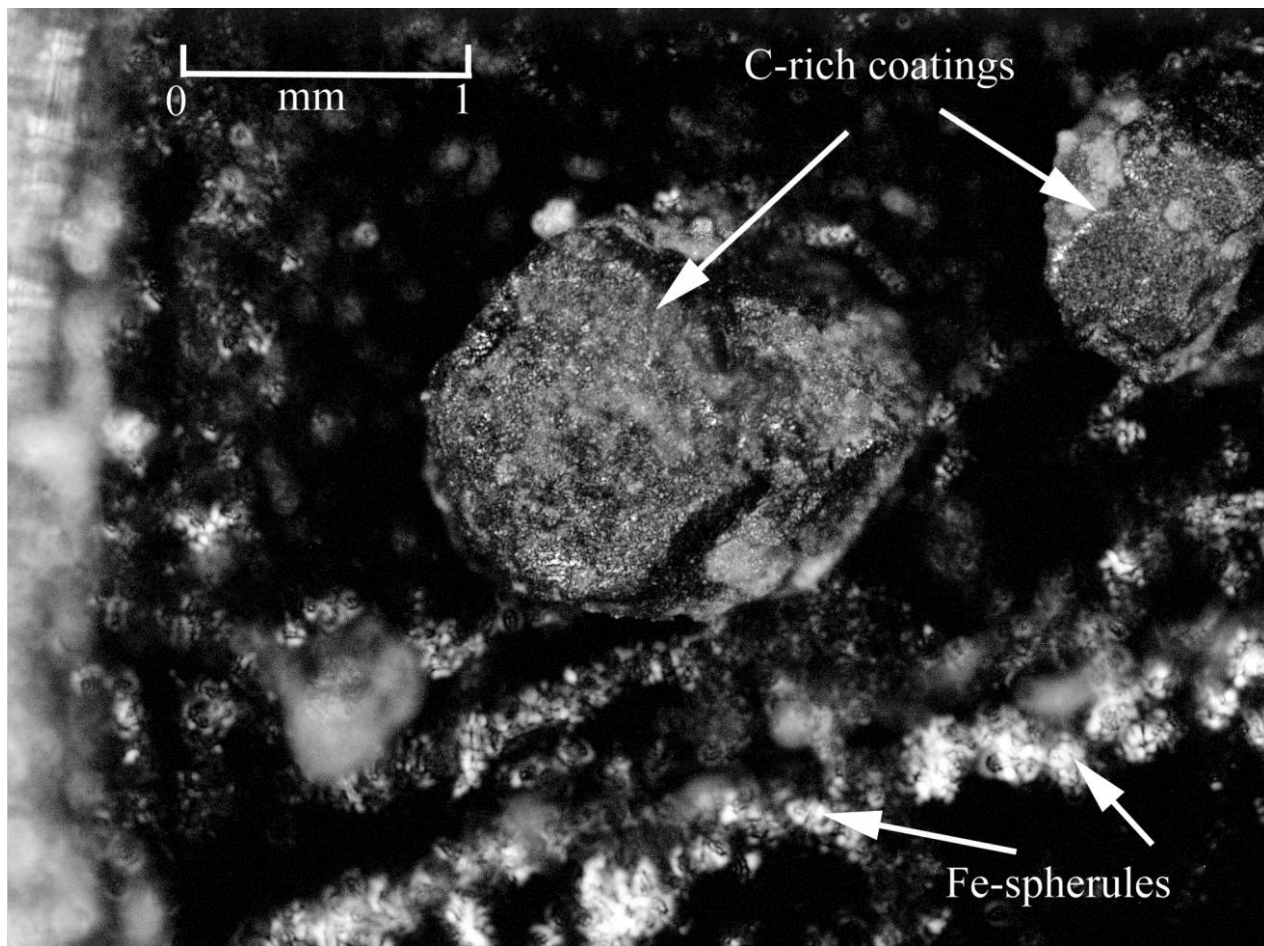


**Figure 3.** Light microscope image of sands from the Ant-828-Cox1 horizon, paleosol cap under the pebble pavement. A color version of this figure is available online.

recovered from the Yucatan impact of 65 Ma (samples from Clear Creek, Colorado; see Mahaney 2002, fig. 11.1C). Shock-melted grains in both frames (figs. 6A, 7A) carry rhyolite and microcline signatures (chemistry in figs. 6B, 7B), most probably sourced from the Antarctic craton, imported by the Inland Ice Sheet, and subjected to an airburst. These individual specimens are single grains rather than the fused clusters often found with other impact/airburst welded-grain assemblages (LeCompte et al. 2012). Grains were observed as individual objects, unlike the Fe-Si spheroids, which are typically found in fused clusters (Mahaney and Keiser 2013). Most grains show distinctive microstructural features (e.g., figs. 6A, 7A) consistent with melting and rapid quenching while airborne. Figure 3 displays “nodular” melt-quenched microforms not exactly reported elsewhere in the literature, although they somewhat resemble YDB spherules reported by LeCompte et al. (2012). Because the grains shown are chemically similar to but morphologically different from melt-quenched spher-

ules, there is uncertainty as to their origin. However, each nodule in figure 3 is ~1–12 mm in diameter, suggesting possible melting of spheroidal clusters or possible postdepositional etching by locally alkaline paleosols. In figure 7A, the fluted shape is consistent with melting and cooling while in flight, and in other instances such grains often carry a tail of melted material (Mahaney et al. 2013a). The fluting on this grain is similar to regmaglypts that are consistent with aerodynamic shaping, as also reported for other YDB spherules by Bunch et al. (2012).

A significant percentage of grains examined in the Cox1 surface horizon (15%) carry circular to near-circular depressions (fig. 8A), likely corrosion features produced by intense heating and fresh by Antarctic standards, as expected, given the dry-cold climate and limited weathering time since the proposed black-mat event. The base of these depressions is shown in this instance to carry melted crystallographic planes of microcline, a micro-house-of-cards-like structure. The EDS in figure 8B confirms a microcline com-

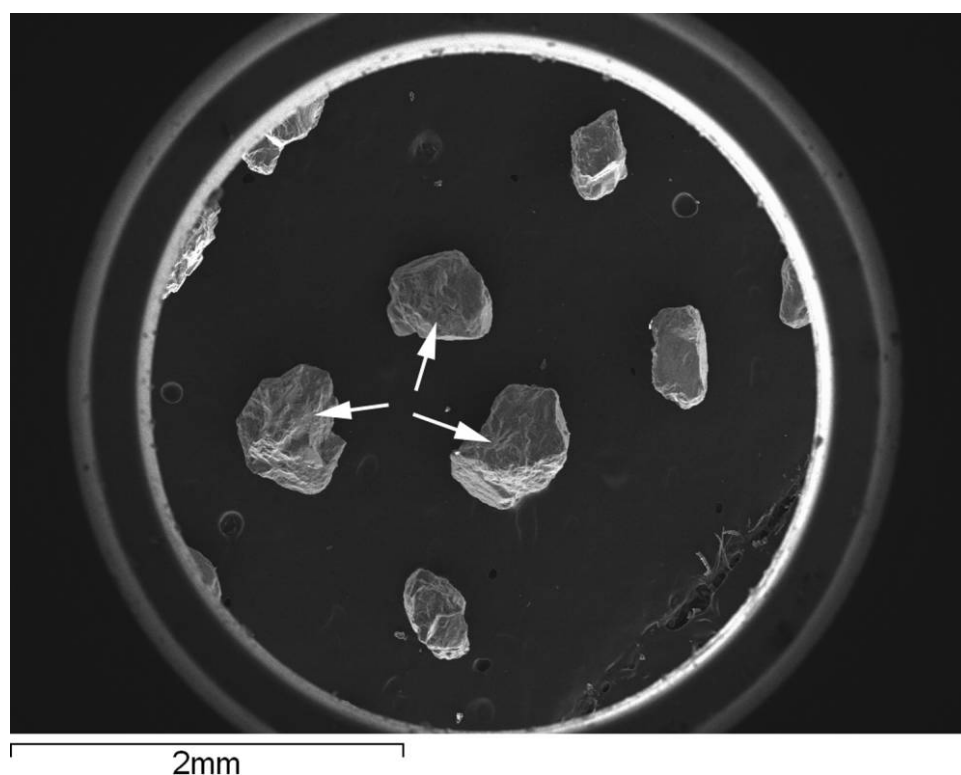


**Figure 4.** Coarse sand fraction grains recovered from Ant-828-Cox1 with predominate angular to subangular features, all with thin to thick Si-Fe coatings. Shrinkage cracks (arrows) in coatings are common on 50% of grains analyzed.

position for the grain in *A* with secondary apatite, possibly the residue of a melted grain, plus Fe coating and appreciable carbon. The carbon would have to be imported, as the surface at the time of impact/airburst was devoid of plant cover. The lack of any impact crater in the area argues for an airburst.

Another microcline grain, shown in figure 9A, contains two solubilized Si streams in two prominent microdepressions on the grain surface, the only probable cause being heating from an airburst. The EDS analysis (fig. 9B) shows a microcline chemistry, again with secondary apatite and Fe coating.

An augite grain in figure 10A, in the Cox2 horizon, shows larger, near-circular depressions, presumed to be corrosion forms of melted grain fabric, all confirmed Si-Al with minor Fe. The grain outside the melted/corrosion microfeature lacks carbon (area 18; fig. 10B), whereas carbon is present in the melted depression (area 19), suggesting that the carbon was imported and restricted to the heated portion of the mineral. The lack of MgO enrichment makes the grain dissimilar to 95% of glassy cosmic spherules (Bunch et al. 2012). In addition, these melted surfaces are definitely inconsistent

with a volcanic origin, as shown in figure 10C, with appreciable carbon present. On the other hand, these grains plot within the range of terrestrial impact materials (fig. 10C), including other documented spherules, ejecta, and tektites from 12 craters and tektite strewnfields [Chicxulub crater [Hildebrand 1993], the Chesapeake Bay crater, Tunguska, the Australasian tektite field, the Lake Bosumtwi crater, the Ries crater, and more [data from Bunch et al. 2012; Mahaney et al. 2013a]].

Farther downsection in the paleosol complex, grains in the lower horizons show a mix of minerals with cosmic features and by-products, many of which have smaller grains of variable sizes welded onto larger grains mostly consisting of feldspar or quartz, occasionally dolerite and magnetite, many with clusters of spherules that most likely are a mix of terrestrial and cosmic fallout. Very occasionally, buckyball-like grains (fig. 11) have been imaged throughout the lower horizons (Cz2 in this case), but without chemical mapping to search for Pt metals and REEs plus other components of meteor ablation or airburst, such as Ni, Cu, and Cr. The ovoid shape is considered to result from aerodynamic shaping and,

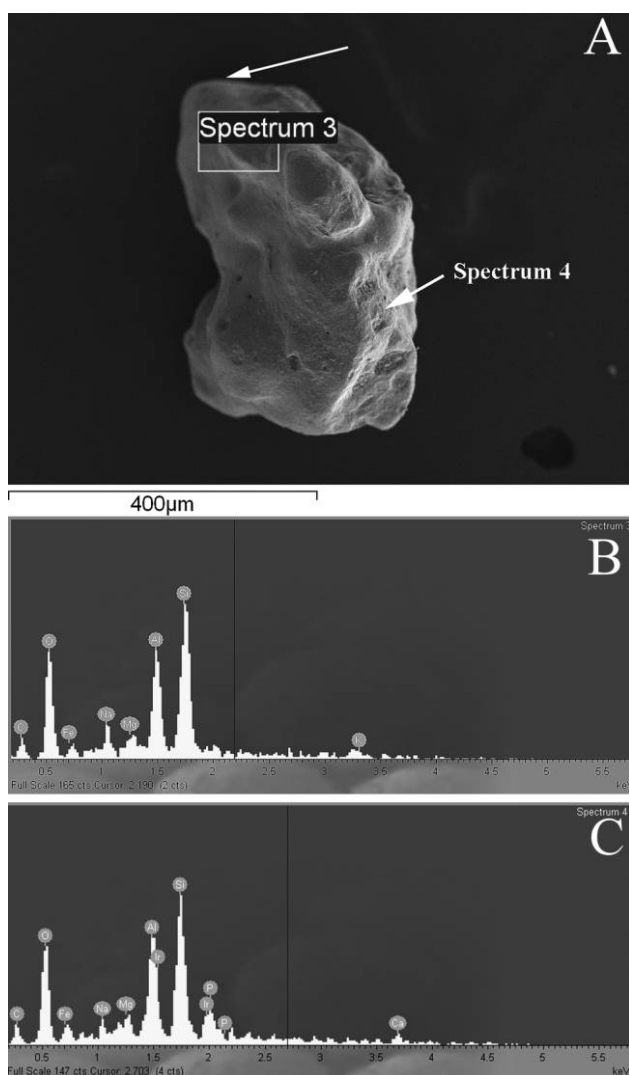


**Figure 5.** A, Representative subangular coarse sand with smoothed-over reformed/melted microfeatures with mapped spectrum (area 3) and point spectrum (area 4). B, Spectrum 3 carries an albite signature with minor Fe and Mg coatings. Carbon is the conductive coating. C, Spectrum 4 reveals a similar albite signature but with a heavier coating of Ca, Mg, Fe, P, and Ir, the latter Pt-group metal an unusual element to detect with the scanning electron microscope/energy-dispersive spectrometer and in considerable concentration. A color version of this figure is available online.

given the similarity to the image in figure 9 of Mahaney et al. (2013a), from the Andean black mat; however, this grain is rather larger and within the fine-sand fraction. Such grains are infrequently scattered through the Ant-828 surface profile, and two examples shown in figures 12 and 13 are representative of plagioclase and orthoclase grains, well coated with Fe and C, with the carbon derived from

the impact/airburst effects or from a previous mid-Miocene tundra environment described by Warny et al. (2009) and Mahaney (2015).

**REEs.** The REEs in Ant-828 (table 1), from light to heavy elements, show a distributional range that parallels REE concentrations in samples from the Western Alps (Mahaney et al. 2016b), in that within the light REEs (La–Sm), only Nd highlights concentrations above crustal averages (Rudnick and Gao 2005), and only in the Cox1 and Cox2 horizons. Within the heavy REEs, Eu is elevated in the Cox2 horizon only, whereas Tb, Yb, and Lu are elevated throughout the surface profile and in selective horizons within the lower (2) profile, the latter possibly related to transference within the tills or residue from a previous impact/airburst. Thorium concentration is well below crustal averages in all horizons of the three profiles in the Ant-828 section.

**Platinum/Pd.** Distributions of Pt/Pd in the three paleosols (table 1) are shown with respect to crustal averages of meteorite-comet airburst/impact and alpine platinum-group-element-rich rocks. The higher Pt/Pd ratios are in the surface paleosol, with the highest values in the Cox group of horizons and somewhat lower values in the salt-rich weathering zones. Within the middle paleosol (unit 2), the higher values are in the 2Cox and 2Cz1 horizons. In the lowest paleosol in the succession, unit 3, values are similar to those in unit 2. While some horizons are consistent with crustal averages for Pt/Pd, others, particularly within the Cox horizons of unit 1, exceed by a small margin the averages for crustal rocks and are barely within the range of a meteorite impact and/or an airburst. The higher concentration of Pt in unit 1 coincides with a wealth of melted/welded/carbon fused grains, as discussed above.

**Taylor Ice Dome.** Cores recovered from the Taylor Ice Dome by Brook et al. (2015) reveal variable concentrations of CH<sub>4</sub>, CO<sub>2</sub>, δ<sup>13</sup>C-CO<sub>2</sub>, and δ<sup>15</sup>N-N<sub>2</sub>O, with increased concentrations of CO<sub>2</sub> and NO<sub>x</sub> dated to 12.9 ka (fig. 14), the precise time of the collision of the comet Encke and Earth that generated the black-mat sediment seen worldwide. While the Taylor data are interpreted to represent carbon fluxes from ocean biological respiration processes, periodic significant release of CO<sub>2</sub> to the atmosphere may be a common feature of Earth's carbon cycle. It is possible that the 12.9 ka carbon and NO<sub>x</sub> "spikes" seen in recovered ice cores from the Taylor Glacier may have more than an ocean source.

## Discussion

Paleosols as recorders of the black-mat event are rare, and rarer still are paleosols in mountainous

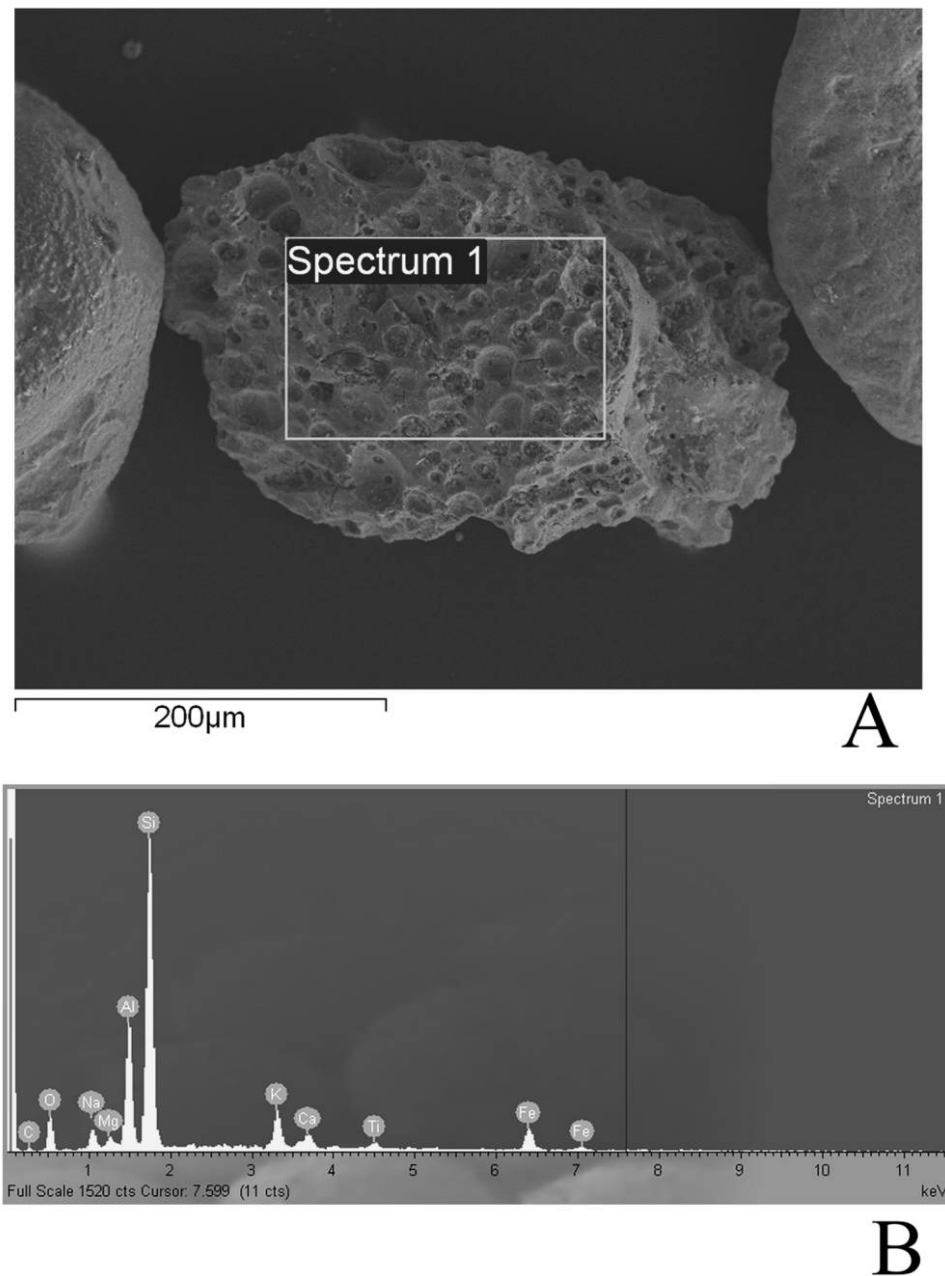


**Figure 6.** *A*, Shock-melted rhyolite bearing a close resemblance to shock-melted quartz from the Yucatan impact; grain recovered from Clear Crick, Colorado (Mahaney 2002, fig. 11.3). The tank and tor microrelief on the grain to left may represent melting of surface. *B*, Energy-dispersive spectral analysis reveals a probable rhyolite with vesicles, with a thin Fe coating. C is the conductive coating.

areas of the world carrying cosmogenic archival evidence. Evidence of the Late Glacial (LG) cosmic collision usually occurs as a fine bed (1–3-cm thickness) carrying a 10YR–5YR hue based on soil color (Oyama and Takehara 1970), with black or near-black values and low chroma whether found in lacustrine-fluvial-lacustrine sediment or in retrieved ice cores. In mountain locales, the black-mat bed may exist

as discrete sediment associated with radiocarbon-dated fluvial and lacustrine sediment (Mahaney et al. 2013a), as melted/welded minerals in weathering rinds (Mahaney and Keiser 2013; Mahaney et al. 2016a), and/or as dispersed sediment in paleosols, repositioned as a result of normal soil processes operative in postimpact time. In some cases, such cosmic-affected sediment might be reworked by glacial ac-

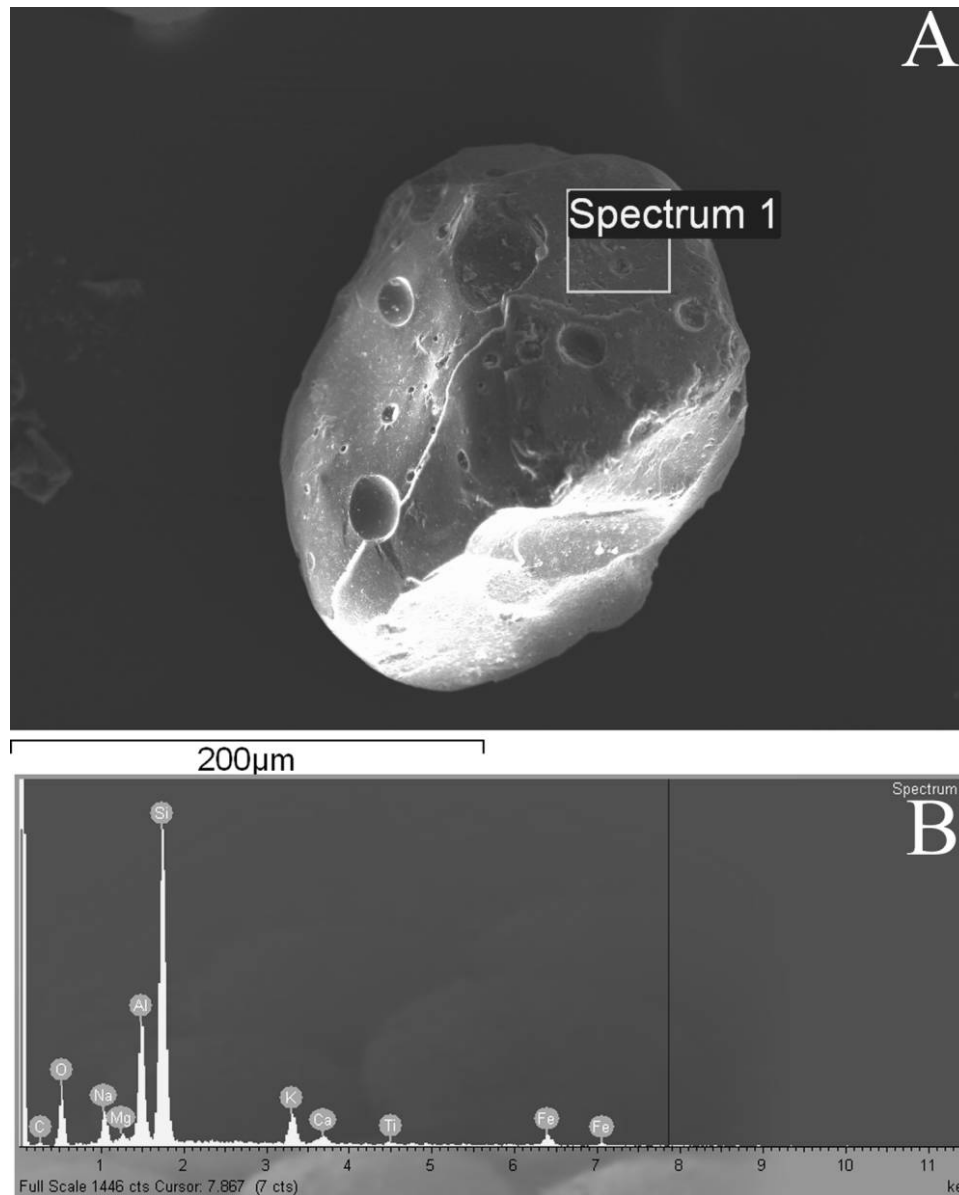


**Figure 7.** *A*, Subround coarse sand carrying a microcline signature with very fresh shock-melted microfeatures including fresh, slightly weathered tanks. *B*, Energy-dispersive spectrometry reveals thin coatings of Fe, Ca, Mg, and Ti.

tivity after the impact/airburst. In all cases in the mountains thus far, evidence related to the YDB (12.8 ka) has been recovered either in situ with little reworking or translocated within paleosols.

**Western Alps.** As with the Ant-828 section discussed here, the G3 site in the Western Alps (Mahaney et al. 2013b, 2016b), located on the inner LG recessional moraine of the upper Guil River valley of France, is situated such that it received sufficient heat to melt outer clast surfaces, presumably from the full force of a cosmic airburst cover-

ing an indeterminate area of the French and Italian Alps. As with the Antarctic samples, the exact time frame is unknown because of a lack of  $^{14}\text{C}$  controls, but the mid-LG age of the G3 site places it within  $\pm 300$  y of the YDB and in a location nearly overrun by younger end moraines considered to be of YD age (Mahaney et al. 2016b). Unlike the Guil River site, where precise dating is not possible, an ice lens in the Taylor Ice Dome (Brook et al. 2015) dated to 12.9 ka (fig. 13) presents the likelihood of a cross correlation between Ant-828 and the YDB.

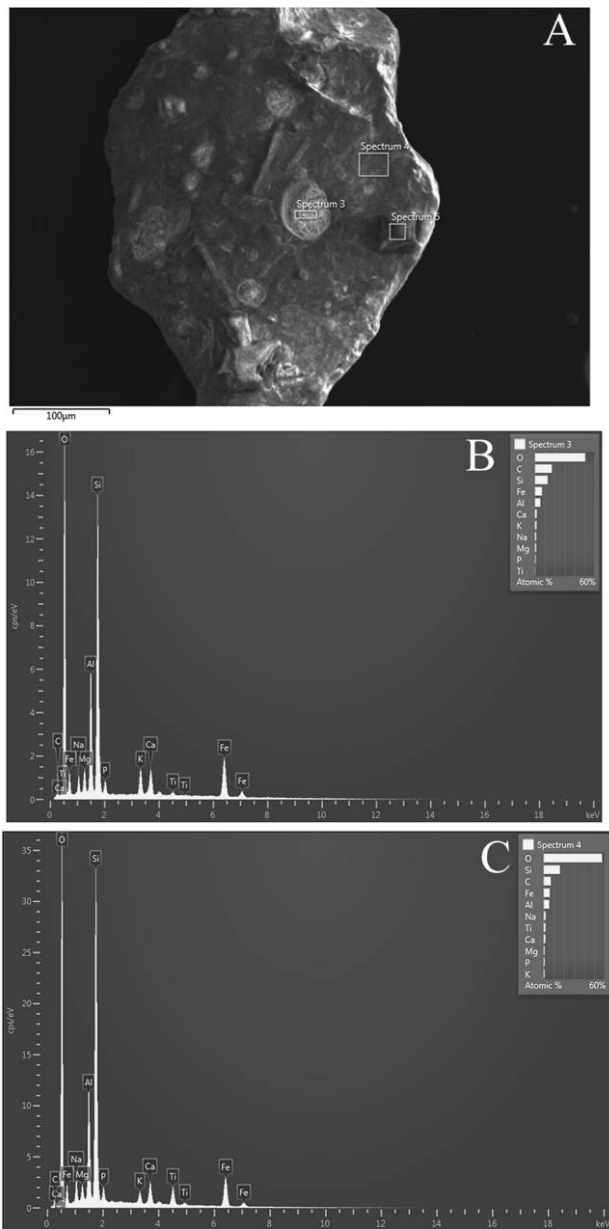


**Figure 8.** *A*, Near-circular depressions in feldspar, an apparent corrosion features possibly produced by intense heating. *B*, Enlargement (energy-dispersive spectrometry [EDS], area 3) showing detail of melted/welded crystallographic planes of microcline, a microstack of cards buried in a shock-melted cavity with more carbon than in *C*. *C*, EDS 4 of the area around a circular depression, showing a probable microcline composition with apatite, Fe as coating, and carbon, the latter retained either from source rock in place or direct from the proposed airburst. Alternatively, if this carbon is not from the black mat, then possibly it is from a carbonaceous chondrite or even a false positive.

The Guil River (G3) site is undeniably correlated with a reversal of the warming event of the Bølling-Allerød climatic forcing. What is certain in the Western Alps is that a glacial resurgence, presumably during the YD cooling interval, emplaced a crosscutting end moraine that partially buried the mid-LG moraine, creating a small tarn, now filled with coarse clastic debris from talus and debris flows, as outlined by Mahaney et al. (2016b). While an airburst in the Western Alps would have had a major impact on retreating ice, notably changing negative to positive mass-balance conditions and thus affecting ice dynamics leading to the YD resurgence, what is certain in the Antarctic is that such a hypothesized airburst may have had little effect on the inland ice or contributed to the YD with increased ice accumulation.

The YD onset in the Alps began at the upper end of a warming trend that began at 14.7 ka (van der Hammen and Hooghiemstra 1995; Teller et al. 2002; Lowe et al. 2008), with maximum cooling

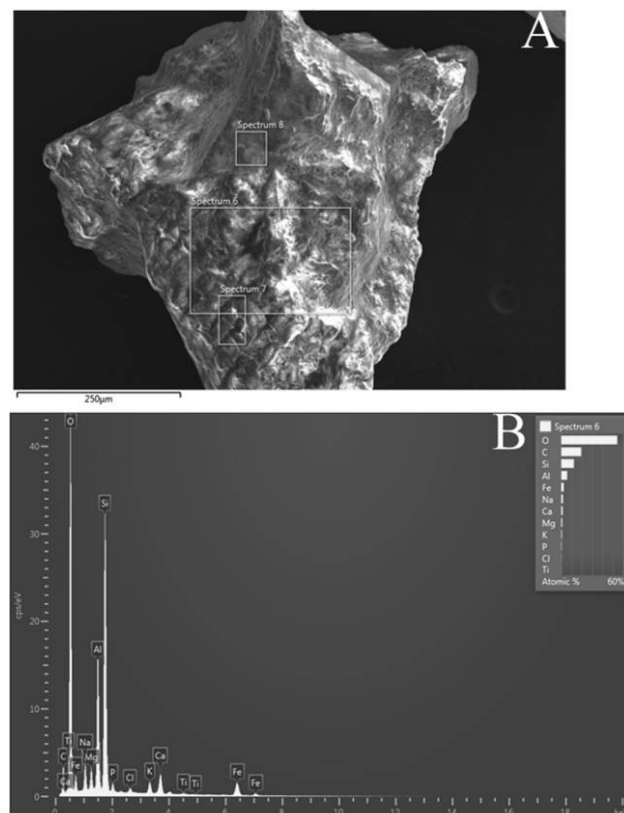


**Figure 9.** *A*, Probable microcline with solubilized fabric. *B*, Energy-dispersive spectrometry (area 6) showing microcline chemistry with minor apatite and Fe coating. The Cl may be cosmic, mixed with or accompanying layers of Fe, the Cl acting as ion receptors in aluminosilicate glass (Stebbins and Du 2002).

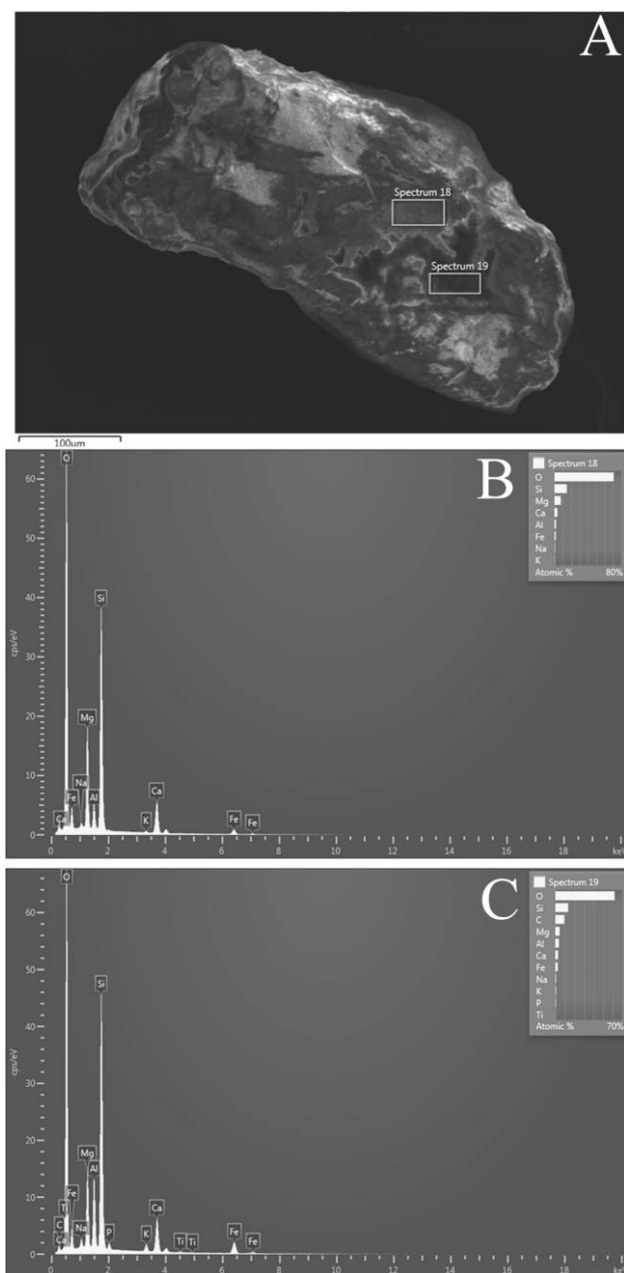


**Figure 10.** A, Augite grain with channels filled with solubilized stream of melted skin, presumably Si. B, Energy-dispersive spectrometry (EDS; area 18) showing the pyroxene skin chemistry. C, EDS (area 19) showing a corrosion depression, possibly the product of intense heat release, with appreciable carbon coating.

beginning at 12.8 ka. The hypothesis that a cosmic airburst could have generated the YD reversal is still hotly debated in the literature (J. P. Kennett et al. 2007; Haynes 2008; Pinter and Ishman 2008; Ge et al. 2009; D. J. Kennett et al. 2009). Recent critical reviews of the YD event by van der Hammen

and van Geel (2008) and Broecker et al. (2010) argue, respectively, that charcoal in paleosols of the Allerød-YD transition were not caused by impact and that the impact event, by itself, could not have caused a glacial advance lasting 1 ky. However, as pointed out by Mahaney et al. (2016b), Earth's encounter with the Taurid meteors following the main event may have been sufficiently strong to maintain a cooling climate and negative mass balance in glaciers around the world. Indeed, YD moraines have been tentatively identified on Mount Kenya by Zreda and Shanahan (2000), but stratigraphic assessment by Mahaney (1990) failed to show ice readvance or cosmic-generated sediment in glacial paleosols, only normal stillstand recession.

The evidence reported here, for both Andean and Alps localities, conclusively contradicts alternative hypotheses for the onset of the YD glacial advance, with the most conclusive evidence coming from aerodynamically modified Fe spherules and microspherules, melted and contorted quartz and other lithologies, and carbon mats welded to various minerals. The presence of technetium, a rare radioactive by-product of uranium fission recovered from the Alps samples, could be a product of a postulated large-scale, if momentary, disruption of the atmosphere, sufficient to allow a cosmic-ray burst. Technetium (atomic number [AN] 43) occupies a position in the periodic table between Mo (AN 42) and Re (AN 44) and has been detected in melted pyroxene in site G3 weathered rind sediment. Because it is a product of atomic-bomb blasts (Yoshihara 2006) and because of its presence in carbon stars (Bernatowicz et al. 2006), Tc might be an undiscovered by-product of a bolide or a comet impact/airburst. Alternatively, it may be an air-influxed contaminant from nuclear reactors (Istok et al. 2004), that is, Chernobyl, or a false positive, as indicated previously (Mahaney and Keiser 2013). Tc was found in only one occurrence in the Alps out of thousands of grains analyzed, indicating that it is not widespread. More work is needed to confirm its presence and determine its origin. Platinum, specifically Pt/Pd, has been found in several mid-LG paleosols of the Guil River of France, with concentrations exceeding crustal averages (Rudnick and Gao 2005). Its variable occurrence in several paleosols is considered to be fallout of cosmic material following ignition near the surface.

**Andean Mountains.** Oriented SW-NE, the bifurcated Mérida Andes extend from the Venezuelan-Colombian border toward the Caribbean coast, occupying a 100-km-wide mountain range with summits reaching 5000 m above sea level (asl; i.e., Humboldt Massif). These mountains formed as a consequence of plate collision (Audemard and Audemard 2002),

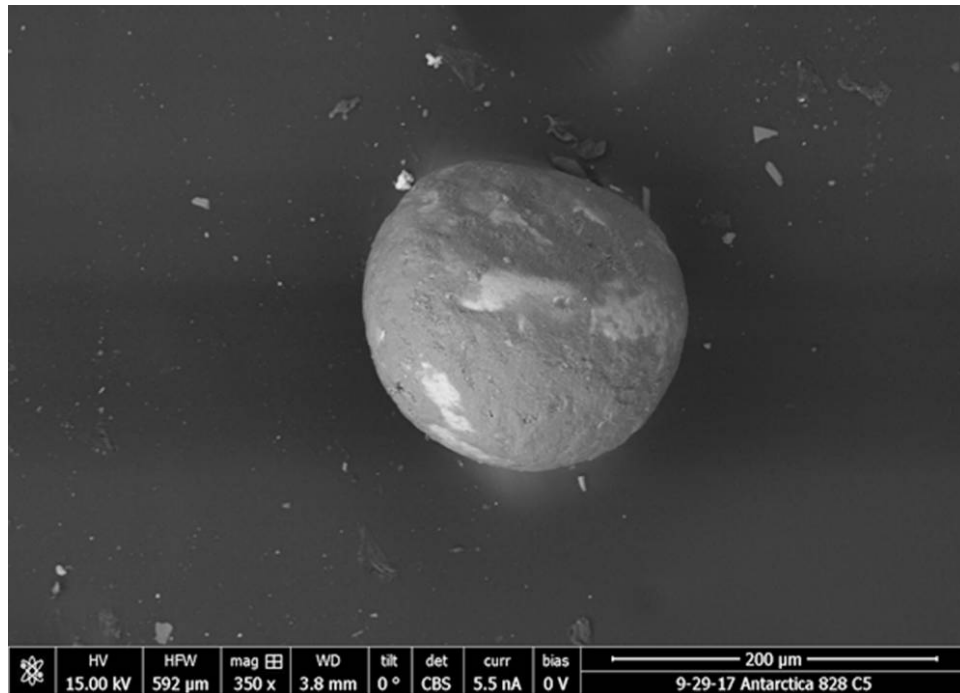


**Figure 11.** Near-ovoid grain similar to buckyball-like mineral agglomerates found in black-mat sediment elsewhere, particularly in the Andes and the Western Alps, all considered to contain welded or fused terrestrial minerals, usually a combination of quartz and plagioclase grains. Despite the plausible cosmic connection, no energy-dispersive spectrum chemistry is available for this specimen. The white areas on the image are probably salts encrusted during post-mid Miocene time.

the onset of orogeny beginning in the late Miocene. The Sierra de Santo Domingo, in which the Mucuñuque catchment is located, along the northeastern limb of the Boconó Fault, is floored with Precambrian bedrock of gneiss and granite of the Iglesias Group (Schubert 1970). The SE-NW-oriented Mucuñuque valley, a fault-controlled, glacially carved valley, descends from elevations above 4200 m on the western slopes of Pico Mifés (4600 m asl) and Pico Mucuñuque (4672 m asl), draining into Lago Mucubaji (ca. 3600 m asl). The Mucuñuque valley drains across the MUM7 and MUM7B sites (Mahaney et al. 2013a) into the Rio Santo Domingo, which follows a long, arcuate drainage emptying into the Orinoco Basin in eastern Venezuela. Upstream of mid-LG recessional moraines (Mahaney et al. 2013a), investigations revealed multiple moraines (site MUM7) comprising mid-LG and YD deposits, with YD outwash fans located upvalley (site MUM7B), the latter burying alluvial peat dated to within the YDB window. The outwash documents the retreat of YD-aged ice, and the MUM7B section, situated at 3800 m asl, contains YDB black-mat sediment with aerodynamically shaped grains (Mahaney et al. 2013a) similar to those described in this report for Ant-828.

**Antarctica.** The Ant-828 deposit having broad overlap well within the time frame of the black-mat sites established elsewhere, and with the normal black-mat grain signature present, it is reasonable to assume that this evidence resulted from the 12.8 ka airburst. There is no other proposed cosmic event that falls within the LG time frame. We cannot conclusively correlate the airburst evidence with the LG period, but the presence of a cosmic signature in weathered sand surfaces from the Cox1 and associated horizons of the Ant-828 paleosol epipedon suggests that the airburst event is possibly coeval with the C/N-rich lens in the Taylor Dome. The C/N evidence of Brook et al. (2015), hypothesized to be related to biologic resurgence in a warming ocean, may, in fact, be at least partially related either to biomass burning (Wolbach et al. 2018a) or to a cosmic event and presumably, given the absence of a crater, to an airburst. The carbon imaged on sands in Ant-828 may presumably be the product of an airburst or resulting wildfire at an unknown location that created carbon welded to heated and melted materials. Presumably, the hypothesized Antarctic airburst was similar to the progenitor of the YD climatic reversal in the Alps and the Andes, the latest event in the LG record (Litt

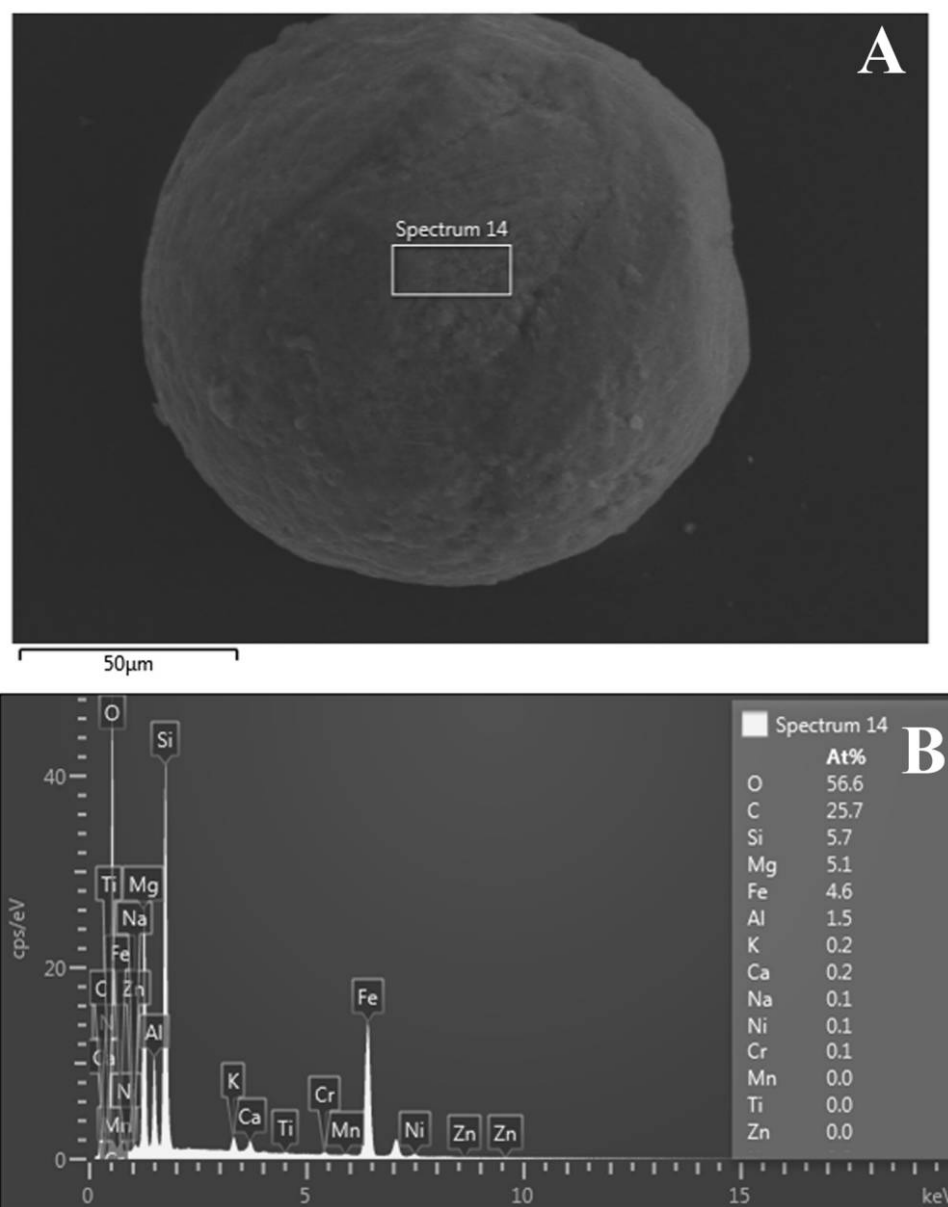


**Figure 12.** *A*, Welded grain in the Ant-828-Cz2 horizon. *B*, Energy-dispersive spectrometry indicates probable plagioclase with Fe minerals, possibly biotite and hematite. Trace amounts of Ni, Cr, and some Fe may be from cosmic sources. Carbon may be from the proposed airburst or possibly from the tundra environment that existed here during the mid-Miocene. The welded character of the grain dendritic texture is similar to forms identified in the Andean black mat of Mahaney et al. (2013a, their fig. 9), the result of melting and air quenching. This example deep in the profile may be a black-mat signature grain or the product of some other impact/airburst or meteor ablation.

et al. 2001; Gibbard 2004). The presence of Ir in the Cox1 horizon of Ant-828 (fig. 5A) is a rare find with the SEM/EDS, an occurrence that supports opaque carbon welded onto felsic grains, the presence of spherules, shock-melted grains, and so on. Moreover, the slightly elevated Pt concentrations in the Cox1 horizons of unit 1 support the hypothesis of either meteor ablation or an airburst at some point in time after the MMCO, the time frame of ~15 Ma for unit 1

exceeding the probable 1-My weathering times for both units 2 and 3 (Mahaney et al. 2001). If aligned with the surface carbon print seen on sands in the Ant-828-Cox1 horizon, it is possible that the Pt concentration therein is related to the 12.9-ka-dated ice layer in the Taylor Ice Dome.

**Testable Hypotheses.** The testable hypothesis used to either support or negate the black-mat occurrence, namely, aqueous sedimentation and some

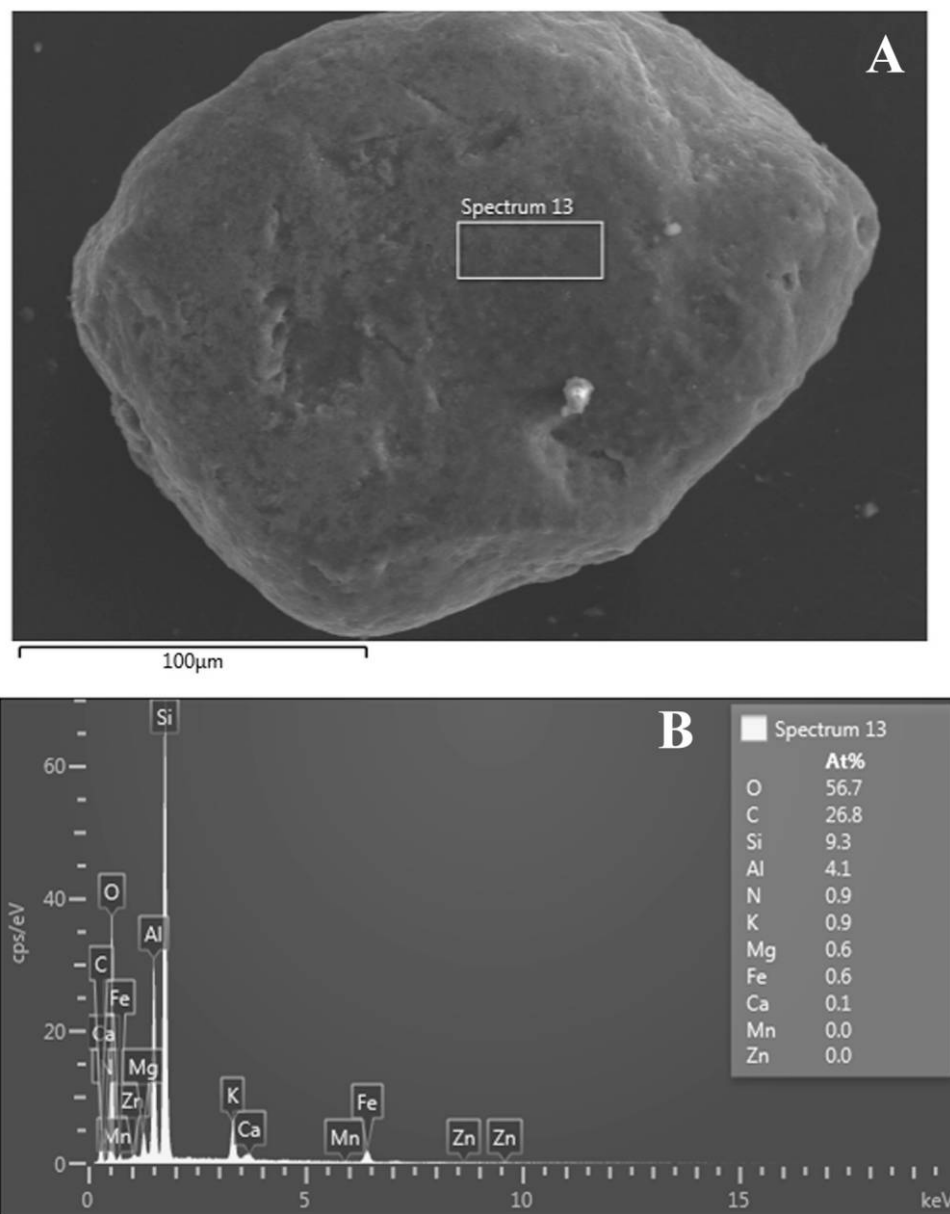


**Figure 13.** A, Probable orthoclase. B, Energy-dispersive spectrometry indicates coatings with stray cations of Ca and Na in the Cz2 horizon of the Ant-828 surface paleosol. The Fe content is coating derived from variable rates of weathering since the mid-Miocene. The carbon may be relict, possibly from the mid-Miocene tundra environment known to have existed for an indeterminate time circa 15 Ma or from the proposed airburst.

form of weathering, has focused on placons (aquifers) requiring a flux of water requiring chemolithotrophic bacteria (Bougerd and de Vrind 1987) and alternating redox conditions producing retention of C, Mn, and Fe without any cosmic influence. Since organic matter is nil and liquid water is in short supply in the Ant-828 section, these hypotheses are not applicable in this case. In support of a black-mat origin for the sediment in Ant-828, it is important to note that of all

the opaque carbon lacing grains in figure 3, the C is on grain surfaces covering much older weathered surfaces and is therefore much younger, possibly aligned with the 12.8 ka age of the YDB. Also, other signature data, such as shock-melted grains and grains with solubilized streams of melted material, appear to be fresh surfaces with little weathering and, despite the dry-cold climate, also of a young age. While not conclusive, the data do point to a close relative age cor-

**Table 1.** Rare Earth Element Concentrations and Pt/Pd in the Ant-828 Paleosol, Antarctica

Horizon	La (ppm)	Ce (ppm)	Nd (ppm)	Sm (ppm)	Eu (ppm)	Tb (ppm)	Yb (ppm)	Lu (ppm)	Th (ppm)	Pt (ppb)	Pd (ppb)	Pt/Pd
Crustal abundance	31	63	27	4.7	1.0	.7	1.96	.31	10.5	.5	.5	1.0
Cox1	19.4	35.4	40.7	3.42	.99	.92	2.76	.45	5.1	2.2	1.4	1.6
Cox2	18.8	36.5	35.8	3.16	1.04	1.03	2.97	.46	5.3	1.3	.7	1.8
Cox3	18.1	34.8	14.9	3.20	.85	.83	2.46	.40	5.5	1.2	1.3	1.0
Cz1	17.5	35.1	9.2	3.20	.81	.75	2.49	.35	4.8	2.3	8.0	.3
Cz2	20.1	36.0	15.0	3.09	.81	.76	2.28	.37	6.5	1.6	2.2	.7
2Cox	19.4	34.5	14.0	3.11	.88	.70	2.28	.32	6.4	2.4	2.2	1.1
2Cz1	32.8	50.7	21.3	4.00	.77	.75	2.76	.39	4.6	2.7	2.0	1.4
2Cz2	22.3	35.9	16.9	3.32	.84	.70	2.23	.31	4.2	3.2	3.6	.9
3Cox	18.4	30.8	20.9	2.83	.84	.63	2.33	.30	4.4	1.6	2.1	.8
3Cz	16.9	28.1	13.2	2.53	.76	.49	1.85	.26	4.5	2.0	1.9	1.1
3Cu	20.2	31.7	12.8	2.69	.79	.56	1.78	.25	3.8	1.9	2.4	.8

relation of sediment in Ant-828 with the 12.9 ka time line of the Taylor Ice Dome record (Brook et al. 2015).

A second alternative hypothesis might question the lack of C-rich spherules in the samples under discussion and the lack of chondrules as an important argument against a cosmic origin. Comparison of the C-rich spherules in the Andean black mat with similar samples analyzed by Firestone et al. (2007a, 2007b) showed more similarities than differences. If one were to consider the C-rich spherules as less dense than those studied by Firestone et al. (2007a), one might also argue that the Andean specimens could have weathered extensively or suffered from distance traveled. While no C-rich spherules were identified in the Antarctic and Alps samples, it is possible that they may have suffered vaporization or that fallout might have preceded terminal delivery, given the greater distances involved. Additional analysis with the scanning transmission electron microscope and FIB may yet reveal the presence of microspherules that would help to bolster a cosmic origin.

A third hypothesis might challenge our assertion that fired sediment underwent extremes of heat without impact, which is entirely possible. However, while low- and high-temperature firing experiments have produced microfractures around grain edges, producing a microbrecciated effect, grains in the Andean black-mat bed (Mahaney et al. 2010, 2011a, 2011b) exhibit a fusion of carbon with quartz. Moreover, the twisted/contorted nature of select grains in the Andean and Alps black mat indicates something more than low-grade temperatures similar to a bush fire or higher-grade lightning strike occurring at the affected sites. Even considering the partial evidence presented here for the Dry Valley samples, a cosmic connection appears to offer a possible explanation.

A fourth hypothesis might involve simple physical weathering as the major source of cracked clasts,

but if this were the case, it would be expected that shock-melted clasts would show similar effects and would carry similar brecciated surfaces connected to internal crack systems. Mechanical weathering could not produce solubilized streams of melted mineral skin, nor could it produce melted and contorted mineral fragments, which are best explained by the high heat and pressure of a cosmic airburst.

Firestone et al. (2007a) proposed that the black-mat impact (YDB) generated microspherules on a grand scale, the combined effect of impactor ablation and high-temperature melting of terrestrial target

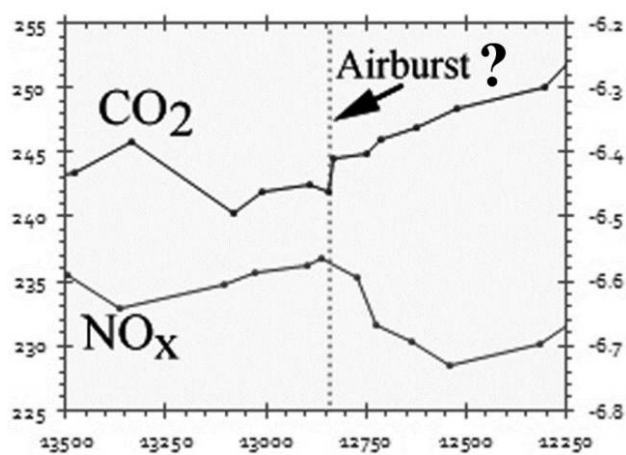


**Figure 14.** Concentrations of CO<sub>2</sub> and NO<sub>x</sub> from the Taylor Glacier blue ice archive dated to 12.9 ka, from Brook et al. (2015) and Marcott et al. (2014), adapted from figure 7 in Wolbach et al. (2018a), probably reflect worldwide biomass burning. The C and N concentrations are considered to come from marine and terrestrial sources, but the spike of both elements at 12.9 ka points to a possible airburst from the black-mat cosmic event and certainly fall within the time of the Younger Dryas boundary.

rocks. Here, we discuss the latter possibility, that microspherules either are present in the grapevine-like string of spherules or exist in opaque carbon coatings on some grains, as shown in figure 3. An extraterrestrial event might not have been a bolide but may in fact have been a cometary vehicle (comet Encke) breaking up over southern Canada, as proposed by Napier (2010). As expected with an airburst, a widely turbulent impact plume or fireball would form an incandescent cloud containing vapor largely from the resident Laurentide Glacier, melted rock from within the comet, shocked and unshocked rock debris, breccia, microspherules, and other abiotic impact materials resident in the target area and sent high into the atmosphere. Alternatively, some carbon might be resident within the comet and/or sourced from a fragment or fragments skip-bombing across Central or South America (something akin to the Yucatan impact skip-bombing into Clear Creek, Colorado; Mahaney 2002), ultimately exploding over the Dry Valleys. Commonly, melted siliceous glass (lechatelierite) is formed on impact when plume temperatures reach 2200°C, the boiling point of quartz. Lechatelierite is an impact feature and is not sourced from volcanoes or from metamorphic terrain, but it may be produced by lightning, which also produces fulgurite. That lechatelierite and fulgurite were not observed in the studied sample suite suggests that the firing temperature may not have reached the 2200°C level.

Assuming that a secondary airburst produced the relevant heat and pressure to affect resident sediment, convective cells would be expected to form instantaneously at temperatures similar to or possibly higher than those in the photosphere of the sun (Bunch et al. 2012). Materials within the fireball interact briefly with cloud materials and nearby snow and ice to produce hot vapor and molten phases, some of which may be ejected downward to interact with country rock. Fireballs produced by airbursts are expected to have limited life spans, perhaps in the range of tens of seconds, but may reach high enough into the atmosphere to open a conduit allowing a brief cosmic-ray flux, producing isotopic changes at the surface. The interaction of particles within the plume may involve repeated collisions, the sum of which produces mineral accretions and collision microfeatures, including regmaglypts (similar to the grain in fig. 7A), which in this case could relate to melted fragments of quartz, pyroxene, and olivine reflecting the nature of the country rock. Although microcraters in the landscape are sometimes by-products of cosmic airbursts (Bunch et al. 2012), none have been identified near Ant-828 to this date.

In support of a cosmic origin, the null hypothesis for a terrestrial origin relies on the presence of high frequencies of breccia, most of which is of glacial origin, modified by high heat and pressure; thick carbon encrustations on select grains; grains sometimes intertwined or welded with other mineral grains; extensive microfractures; and occasional crack propagation inward into fresh lithic cores. Shock-melted grains are not manifestly of normal terrestrial processes, but admittedly the lack of nanodiamonds, planar deformation features, and Be isotopes softens the cosmic hypothesis; but then, the distance between primary impact in southern Canada and the terminal zone of ejecta in Antarctica opens the question of dispersal of impact material with increasing distance from the Laurentide Ice Sheet. The spread of ejecta outward from an impact site is hardly expected to reach the receiving area (ejecta reach about five crater radii from an impact; Boslough 2012), but a detached part of the incoming cosmic cometary vehicle could reach the Antarctic Dry Valleys, as interpreted for other airburst fragments that reached the French coast, the French/Italian Alps (Mahaney and Keiser 2013), the northwestern Venezuelan Andes (Mahaney et al. 2013a), the Netherlands (Kloosterman 2007), Abu Hureyra, Syria, central Asia (Bunch et al. 2012), and most recently southern Chile (A. West, personal communication, 2017).

## Conclusions

Paleosols, as long-term recorders of environmental interaction between the lithosphere, the atmosphere, and the biosphere, sometimes contain evidence of signature events such as cosmic impacts and airbursts, all noted in various locales such as the northern Andes, the Western Alps of Europe, and the Antarctic Dry Valleys, the last highlighted here. In this particular case, investigations of Antarctic paleosols with a focus on weathering features led to a realization that the upper horizons of a middle Miocene stratigraphic stack of paleosols served to record evidence of an impact or airburst. Despite the lack of a crater, and considering that meteor ablation or fragment airburst could account for the melted/welded grains imaged in recovered samples, and considering that increased CO<sub>2</sub> and NO<sub>x</sub> concentrations had been recovered in ice cores from the nearby Taylor Ice Dome, all dated to 12.9 ka, the possible correlation of the Ant-828 paleosol sediment to the black-mat airburst dated by Kennett et al. (2015) began to appear as more than a mere coincidence. The data comprising strings of spherules, carbon-coated felsic grains, melted/welded grains of

variable lithology, solubilized Si streams forming rivulets on grain surfaces, shock-melted grains, and corrosion depressions, Ir in coatings verified by EDS, and Pt/Pd ratios elevated above crustal averages all point to evidence of a cosmic collision, unprecedented in the slim research record of Antarctic paleosols. What is unclear is whether grains in the lower horizons of Ant-828 are related to the black-mat event or to some previous meteor ablation, impact, or airburst. All the more important is the conclusion that paleosols may contain unprecedented paleoenvironmental records that need to be mined by

young minds entering into geological/geomorphological investigations.

#### ACKNOWLEDGMENTS

This research was funded by Quaternary Surveys, Toronto. W. C. Mahaney gratefully acknowledges support from the New Zealand Antarctic Programme, KIWI-105 event (1998). We gratefully acknowledge criticism and useful comment from A. Fairén (European Space Agency, Madrid) and an anonymous reviewer.

#### REFERENCES CITED

- Anderson, J. B.; Warny, S.; Askin, R. A.; Wellner, J. S.; Bohaty, S. M.; Kirshner, A. E.; Livsey, D. N.; et al. 2011. Progressive Cenozoic cooling and the demise of Antarctica's last refugium. *Proc. Natl. Acad. Sci. USA* 108(28):11,356–11,360.
- Armstrong, R. L. 1978. K-Ar dating: late Cenozoic McMurdo volcanics and Dry Valley glacial history. *N. Z. J. Geol. Geophys.* 21:685–698.
- Audemard, F. E., and Audemard, F. A. 2002. Structure of the Mérida Andes: relations with the South America–Caribbean geodynamic interaction. *Tectonophysics* 345:299–327.
- Barrett, P. J. 1981. History of the Ross Sea region during the deposition of the Beacon Supergroup 400–180 million years ago. *J. R. Soc. N.Z.* 11:447–458.
- Bernatowicz, T. J.; Croat, T. K.; and Daulton, T. L. 2006. Origin and evolution of carbonaceous presolar grains in stellar environments. In Lauretta, D. S., and McSween, H. Y., Jr., eds. *Meteorites and the early solar system II*. Tucson, University of Arizona Press, p. 109–126.
- Birkeland, P. W. 1999. *Soils and geomorphology*. Oxford, Oxford University Press, 430 p.
- Bo, S.; Siegert, M. J.; Mudd, S. M.; Sugden, D.; Fujita, S.; Cui, X.; Jiang, Y.; Tang, X.; and Li, Y. 2009. The Gamburtsev mountains and the origin and early evolution of the Antarctic Ice Sheet. *Nature* 459:690–693. doi:10.1038/nature08024.
- Bockheim, J. G. 2007. Soil processes and development rates in the Quartermain Mountains, upper Taylor Glacier region, Antarctica. *Geogr. Ann.* A 89:153–165.
- . 2013. Paleosols in the Transantarctic Mountains: indicators of environmental change. *Solid Earth Discuss.* 5:1007–1029.
- Boslough, M. 2012. Inconsistent impact hypotheses for the Younger Dryas. *Proc. Natl. Acad. Sci. USA* 109(34):E2241. doi:10.1073/pnas.1206739109.
- Bougerd, F. C., and de Vrind, J. M. P. 1987. Manganese oxidation by *Leptothrix discophora*. *J. Bacteriol.* 169:489–494.
- Bradshaw, M. 2013. The Taylor Group (Beacon Supergroup): the Devonian sediments of Antarctica. In Ham-
- brey, M. J.; Barker, P. F.; Barrett, P. J.; Bowman, V.; Davies, B.; Smellie, J. L.; and Tranter, M., eds. *Antarctic palaeoenvironments and Earth-surface processes*. *Geol. Soc. Lond. Spec. Publ.* 381:67–97. doi:10.1144/SP381.23.
- Broecker, W. S.; Denton, G. H.; Edwards, R. L.; Cheng, H.; Alley, R. B.; and Putnam, A. E. 2010. Putting the Younger Dryas cold event into context. *Quat. Sci. Rev.* 29:1078–1081.
- Brook, E. J.; Bauska T.; and Mix, A. 2015. Isotopic constraints on greenhouse gas variability during the last deglaciation from blue ice archives. In Sarinthein, M., and Haug, G. H., eds. *Deglacial changes in ocean dynamics and atmospheric CO<sub>2</sub>*. *Nova Acta Leopold., N.F.*, 121(408):39–42.
- Bunch, T. E.; Hermes, R. E.; Moore, A. M. T.; Kennett, D. J.; Weaver, J. C.; Wittke, J. H.; DeCarli, P. S.; et al. 2012. Very high-temperature impact melt products as evidence for cosmic airbursts and impacts 12,900 years ago. *Proc. Natl. Acad. Sci. USA* 109(28):E1903–E1912.
- Campbell, I. B., and Claridge, G. G. C. 1987. *Antarctica: soils, weathering processes and environment*. Amsterdam, Elsevier, 368 p.
- Claridge, G. G. C. 1977. The salts in Antarctic soils, their distribution and relationship to soil processes. *Soil Sci.* 123:377–384.
- Claridge, G. G. C., and Campbell, I. B. 1968. Origin of nitrate deposits. *Nature* 217:428–430.
- Cuffey, K. M.; Conway, H.; Gades, A. M.; Hallet, B.; Lorrain, R.; Severinghaus, J. P.; Steig, E. J.; Vaughn, B.; and White, J. W. C. 2000. Entrainment at cold glacier beds. *Geology* 28(4):351–354.
- Denton, G. H.; Anderson, R. F.; Toggweiler, J. R.; Edwards, R. L.; Schaefer, J. M.; and Putnam, A. E. 2010. The last glacial termination. *Science* 328(5986):1652–1656.
- Ferrar, H. T. 1907. Report on the field-geology of the region explored during the *Discovery* Antarctic Expedition 1901–4. In *National Antarctic Expedition 1901–1904*. *Geology*. Vol. 1 of *Natural history*, p. 1–100.
- Firestone, R. B.; West, A.; Kennett, J. P.; Becker, L.; Bunch, T. E.; Revay, Z. S.; Schultz, P. H.; et al. 2007a. Evidence

- for an extraterrestrial impact 12,900 years ago that contributed to the megafaunal extinctions and the Younger Dryas cooling. *Proc. Natl. Acad. Sci.* 104: 16,016–16,021.
- Firestone, R. B.; West, A.; Revay, Z.; Belgya, T.; Smith, A.; and Que Hee, S. S. 2007*b*. Evidence for a massive extraterrestrial airburst over North America 12.9 ka ago. *EOS: Trans. Am. Geophys. Union* 88(23), Joint Assembly suppl., abstract PP41A-01.
- Ge, T.; Courty, M. M.; and Guichard, F. 2009. Field-analytical approach of land-sea records for elucidating the Younger Dryas syndrome. *EOS: Trans. Am. Geophys. Union* 90(52), Fall Meeting suppl., abstract PP31D-1390.
- Gibbard, P. L. 2004. Quaternary. . . now you see it, now you don't. *Quat. Perspect.* 14:89–91.
- Graham, I. J.; Ditchburn, R. G.; Claridge, G. G. C.; Whitehead, N. E.; Zondervan, A.; and Sheppard, D. S. 2002. Dating Antarctic soils using atmosphere-derived <sup>10</sup>Be and nitrate. *In* Gamble, J. A.; Skinner, D. N. B.; and Henrys, S., eds. *Antarctica at the close of a millennium: proceedings of the 8th International Symposium on Antarctic Earth Sciences*. Wellington, Royal Society of New Zealand, p. 429–436.
- Hancock, R. G. V. 1984. On the source of clay used for Cologne Roman pottery. *Archaeometry* 26:210–217.
- Harrison, T. P., and Hancock, R. G. V. 2005. Geochemical analysis and sociocultural complexity: a case study from early Iron Age Megiddo (Israel). *Archaeometry* 47:705–722.
- Haynes, C. V., Jr. 2008. Younger Dryas “black mats” and the Rancholabrean termination in North America. *Proc. Natl. Acad. Sci. USA* 105:6520–6525.
- Hildebrand, A. R. 1993. The Cretaceous/Tertiary boundary impact (or the dinosaurs didn't have a chance). *J. R. Astron. Soc. Can.* 87:77–117.
- Hodgson, J. M. 1976. Soil survey field handbook. Soil Survey Tech. Monogr. 5. Herpenden, UK, Rothamsted Experimental Station, 99 p.
- Istok, J. D.; Senko, J. M.; Krumholz, L. K.; Watson, D.; Bogle, M. A.; Peacock, A.; Chang, Y.-J.; and White, D. C. 2004. In situ bioreduction of technetium and uranium in a nitrate-contaminated aquifer. *Environ. Sci. Technol.* 38:468–475.
- Kennett, D. J.; Kennett, J. P.; West, A.; Mercer, C.; Que Hee, S. S.; Bement, L.; Bunch, T. E.; Sellers, M.; and Wolbach, W. S. 2009. Nanodiamonds in the Younger Dryas boundary sediment. *Science* 323:94.
- Kennett, J. P.; Becker, L.; and West, A. 2007. Triggering of the Younger Dryas cooling by extraterrestrial impact. *EOS: Trans. Am. Geophys. Union* 88(23), Joint Assembly suppl., abstract PP41A-05.
- Kennett, J. P.; Kennett, D. J.; Culleton, B. J.; Tortosa, J. E. A.; Bischoff, J. L.; Bunch, T. E.; Daniel, I. R.; et al. 2015. Bayesian chronological analyses consistent with synchronous age of 12,835–12,735 cal B. P. for Younger Dryas boundary on four continents. *Proc. Natl. Acad. Sci. USA* 112:E4344–E4353. doi:10.1073/pnas.1507146112.
- Kloosterman, J. B. 2007. Correlation of the late Pleistocene Usselo Horizon (Europe) and the Clovis Layer (North America). *EOS: Trans. Am. Geophys. Union* 88(23), Joint Assembly suppl., abstract PP43A-02.
- LeCompte, M. A.; Goodyear, A. C.; Demitroff, M. N.; Batchelor, D.; Vogel, E. K.; Mooney, C.; Rock, B. N.; and Seidel, A. W. 2012. An independent evaluation of conflicting microspherule results from different investigations of the Younger Dryas impact hypothesis. *Proc. Natl. Acad. Sci. USA* 106(44):E2960–E2969. doi:10.1073/pnas.1208603109.
- Lewis, A. R.; Marchant, D. R.; Ashworth, A. C.; Hemming, S. R.; and Machlus, M. I. 2007. Major middle Miocene global climate change: evidence from East Antarctica and Transantarctic Mountains. *Geol. Soc. Am. Bull.* 119:1449–1461.
- Litt, T.; Brauer, A.; Goslar, T.; Merkt, J.; Bałaga, K.; Müller, H.; Ralska-Jasiewiczowa, M.; Stebich, M.; and Negendank, J. F. W. 2001. Correlation and synchronisation of Lateglacial continental sequences in northern central Europe based on annually laminated lacustrine sediments. *Quat. Sci. Rev.* 20:1233–1249.
- Lowe, J. J.; Rasmussen, S. O.; Björck, S.; Hoek, W. Z.; Steffensen, J. P.; Walker, M. J. C.; and Yu, Z. C. 2008. Synchronisation of palaeoenvironmental events in the North Atlantic region during the Last Termination: a revised protocol recommended by the INTIMATE group. *Quat. Sci. Rev.* 27:6–17.
- Mahaney, W. C. 1990. Ice on the equator. Ellison Bay, WI, Caxton, 386 p.
- . 2002. Atlas of sand grain surface textures and applications. Oxford, Oxford University Press, 237 p.
- . 2015. Pedological iron/Al extracts, clast analysis and Coleoptera from Antarctic paleosol 831: evidence of a middle Miocene or earlier climatic optimum. *J. Geol.* 123:113–132.
- Mahaney, W. C.; Dohm, J. M.; Baker, V. R.; Newsom, H. E.; Malloch, D.; Hancock, R. G. V.; Campbell, I.; Sheppard, D.; and Milner, M. W. 2001. Morphogenesis of Antarctic paleosols: Martian analogue. *Icarus* 154:113–130.
- Mahaney, W. C.; Dohm, J. M.; Kapran, B.; Hancock, R. G. V.; and Milner, M. W. 2009. Secondary Fe and Al in Antarctic paleosols: correlation to Mars with prospect for the presence of life. *Icarus* 203:320–330.
- Mahaney, W. C., and Keiser, L. 2013. Weathering rinds: unlikely host clasts for an impact-induced event. *Geomorphology* 184:74–83.
- Mahaney, W. C.; Keiser, L.; Krinsley, D.; Kalm, V.; Beukens, R.; and West, A. 2013*a*. New evidence from a black mat site in the northern Andes supporting a cosmic impact 12,800 Years Ago. *J. Geol.* 121(6):591–602.
- Mahaney, W. C.; Keiser, L.; Krinsley, D. H.; Pentlavalli, P.; Allen, C. C. R.; Somelar, P.; Schwartz, S.; et al. 2013*b*. Weathering rinds as mirror images of palaeosols: examples from the Western Alps with correlation to Antarctica and Mars. *J. Geol. Soc. Lond.* 170:833–847.
- Mahaney, W. C.; Krinsley, D.; and Kalm, V. 2010. Evidence for a cosmogenic origin of fired glaciofluvial

- beds in the northwestern Andes: correlation with experimentally heated quartz and feldspar. *Sediment. Geol.* 231:31–40.
- Mahaney, W. C.; Krinsley, D.; Langworthy, K.; Hart, K.; Kalm, V.; Tricart, P.; and Schwartz, S. 2011a. Fired glaciofluvial sediment in the northwestern Andes: biotic aspects of the black mat. *Sediment. Geol.* 237:73–83.
- Mahaney, W. C.; Krinsley, D. H.; Dohm, J. M.; Kalm, V.; Langworthy, K.; and Ditto, J. 2011b. Notes on the black mat sediment, Mucuñuque catchment, northern Mérida Andes, Venezuela. *J. Adv. Microsc. Res.* 6:1–9.
- Mahaney, W. C.; Krinsley, D. H.; Razink, J.; Fischer, R.; and Langworthy, K. 2016a. Clast rind analysis using multi-high resolution instrumentation. *Scanning* 38: 202–212. doi:10.1002/sca.21255.
- Mahaney, W. C., and Schwartz, S. 2016. Paleoclimate of Antarctica reconstructed from clast weathering rind analysis. *Palaeogeogr. Palaeoclimatol. Palaeoecol.* 446: 205–212.
- Mahaney, W. C.; Schwartz, S.; Hart, K.; Dohm, J.; and Allen, C. C. R. 2014. Mineralogy, chemistry and biological contingents of an early-middle Miocene Antarctic paleosol and its relevance as a Martian analogue. *J. Planet. Space Sci.* 104:253–269.
- Mahaney, W. C.; Somelar, P.; Dirszowsky, R. W.; Kelleher, B.; Pentlavalli, P.; McLaughlin, S.; Kulakova, A. N.; et al. 2016b. A microbial link to weathering of postglacial rocks and sediments, Mt. Viso area, Western Alps, demonstrated through analysis of a soil/paleosol bio/chronosequence. *J. Geol.* 124:149–169.
- Mahaney, W. C.; Somelar, P.; West, A.; Krinsley, D.; Allen, C. C. R.; Pentlavalli, P.; Young, J. M.; et al. 2017. Evidence for cosmic airburst/impact in the Western Alps archived in Late Glacial paleosols. *Quat. Int.* 438B:68–80. doi:10.1016/j.quaint.2017.01.043.
- Marchant, D. R.; Denton, G. H.; Sugden, D. E.; and Swisher, C. C., III. 1993. Miocene glacial stratigraphy and landscape evolution of the western Asgard Range, Antarctica. *Geogr. Ann. A* 75:303–330.
- Marcott, S. A.; Bauska, T. K.; Buizert, C.; Steig, E. J.; Rosen, J. L.; Cuffey, K. M.; Fudge, T. J.; et al. 2014. Centennial-scale changes in the global carbon cycle during the last deglaciation. *Nature* 514:616–619.
- Meltzer, D. J.; Holliday, V. T.; Cannon, M. D.; and Miller, S. D. 2014. Chronological evidence fails to support claim of an isochronous widespread layer of cosmic impact indicators dated to 12,800 years ago. *Proc. Natl. Acad. Sci. USA* 111:E2162–E2171. doi:10.1073/pnas.1401150111.
- Napier, W. M. 2010. Palaeolithic extinctions and the Taurid Complex. *Mon. Not. R. Astron. Soc.* 405:1901–1906.
- NSSC (National Soil Survey Center). 1995. Soil survey laboratory information manual. Soil Survey Investig. Rep. 45, version 1.00. Lincoln, NE, US Department of Agriculture, 305 p.
- Owen, L. A.; Thackray, G.; Anderson, R. S.; Briner, J.; Kaufman, D.; Roe, G.; Pfeffer, W.; and Yi, C. L. 2009. Integrated research on mountain glaciers: current status, priorities and future prospects. *Geomorphology* 103:158–171.
- Oyama, M., and Takehara, H. 1970. Standard soil color charts. Tokyo, Japan Research Council for Agriculture, Forestry and Fisheries.
- Passchier, S. 2011. Climate change: ancient Antarctic fjords. *Nature* 474:46–47.
- Petaev, M. I.; Huang, S.; Jacobsen, S. B.; and Zindler, A. 2013. Large Pt anomaly in the Greenland ice core points to a cataclysm at the onset of Younger Dryas. *Proc. Natl. Acad. Sci. USA* 110(32):12,917–12,920.
- Pinter, N., and Ishman, S. E. 2008. Impacts, megatsunami, and other extraordinary claims. *GSA Today* 18:37–38.
- Rudnick, R. L., and Gao, S. 2005. Composition of the continental crust. In Rudnick, R. L., ed. *The crust*. Vol. 3 of Holland, H. H., and Turekian, K. K., eds. *Treatise on geochemistry*. Amsterdam, Elsevier, p. 1–64.
- Schubert, C. 1970. Glaciation of the Sierra de Santo Domingo, Venezuelan Andes. *Quaternaria* 13:225–246.
- Shaw, S. E. 1962. Petrography of Beacon sandstone samples from Beacon Height West, upper Taylor Glacier, Antarctica. *N.Z. J. Geol. Geophys.* 5:733–739.
- Soil Survey Staff. 1999. Soil taxonomy. *Agric. Handb.* 436. Washington, DC, US Department of Agriculture, Natural Resources Conservation Service.
- Stebbins, J. F., and Du, L.-S. 2002. Chloride ion sites in silicate and aluminosilicate glasses: a preliminary study by <sup>35</sup>Cl solid state NMR. *Am. Mineral.* 87:359–363.
- Stewart, D. 1934. Petrography of the Beacon sandstone of South Victoria Land. *Am. Mineral.* 19:351–359.
- Teller, J. T.; Leverington, D. W.; and Mann, J. D. 2002. Freshwater outbursts to the oceans from glacial Lake Agassiz and their role in climate change during the last deglaciation. *Quat. Sci. Rev.* 21:879–887.
- Ugolini, F. C., and Anderson, D. M. 1973. Ionic migration and weathering in frozen Antarctic soils. *Soil Sci.* 115:461–470.
- van der Hammen, T., and Hooghiemstra, H. 1995. The El Abra stadial, a Younger Dryas equivalent in Colombia. *Quat. Sci. Rev.* 14:841–851.
- van der Hammen, T., and van Geel, B. 2008. Charcoal in soils of the Allerød-Younger Dryas transition were the result of natural fires and not necessarily the effect of an extra-terrestrial impact. *Neth. J. Geosci.* 87:359–361.
- Warny, S.; Askin, R. A.; Hannah, M. J.; Mohr, B. A. R.; Raine, J. I.; Harwood, D. M.; Florindo, F.; and the SMS Science Team. 2009. Palynomorphs from a sediment core reveal a sudden remarkably warm Antarctic during the middle Miocene. *Geology* 37(10):955–958.
- Wilson, A. T. 1973. The great antiquity of some Antarctic landforms—evidence for an Eocene temperate glaciation in the McMurdo region. In E. M. v. Z. Bakker, ed. *Palaeoecology of Africa*. Vol. 8. Cape Town, Balkema, p. 23–35.
- Wittke, J. H.; Weaver, J. C.; Bunch, T. E.; Kennett, J. P.; Kennett, D. J.; Moore, A. M. T.; Hillman, G. C., et al. 2013. Evidence for deposition of 10 million tonnes of impact spherules across four continents 12,800 y ago. *Proc. Natl. Acad. Sci. USA* 110(23):E2088–E2097. doi:10.1073/pnas.1301760110.

- Wolbach, W.; Ballard, J. P.; Mayewski, P. A.; Adedeji, V.; Bunch, T. E.; Firestone, R. B.; French, T. A.; et al. 2018*a*. Extraordinary biomass-burning episode and impact winter triggered by the Younger Dryas cosmic impact ~12,800 years ago. 1. Ice cores and glaciers. *J. Geol.* 126:165–184.
- Wolbach, W.; Ballard, J. P.; Mayewski, P. A.; Parnell, A. C.; Cahill, N.; Adedeji, V.; Bunch, T. E.; et al. 2018*b*. Extraordinary biomass-burning episode and impact winter triggered by the younger Dryas cosmic impact ~12,800 years ago. 2. Lake, marine, and terrestrial sediments. *J. Geol.* 126:185–205.
- Wynn-Williams, D. D., and Edwards, H. G. M. 2000. Proximal analysis of regolith habitats and protective biomolecules in site by Raman spectroscopy: overview of terrestrial Antarctic habitats and Mars analogy. *Icarus* 144 (2):486–503.
- Yoshihara, K. 2006. Technetium in the environment. *In* Yoshihara, K., and Omori, T., eds. Technetium and rhenium: their chemistry and its applications. Topics in current chemistry. Vol. 176. Berlin, Springer, p. 17–35.
- Zreda, M., and Shanahan, T. M. 2000. Chronology of Quaternary glaciations in East Africa. *Earth Planet. Sci. Lett.* 177:23–40.